NOVEL SURGICAL AND IMAGING METHODS OF THE MIDDLE EAR AND TEMPORAL BONE

Lauri Peltonen, MD

Department of Otorhinolaryngology,
University of Helsinki and Helsinki University Central Hospital,
Helsinki, Finland

ACADEMIC DISSERTATION

To be publicly discussed with the permission of the Medical Faculty of the University of Helsinki in the Great Auditorium, Haartman Institute, on June 6, 2008, at 12 noon

Helsinki 2008

ISBN: 978-952-92-3622-0 (paperback)
ISBN: 978-952-10-4618-6 (PDF)
http://ethesis.helsinki.fi
Yliopistopaino
Helsinki 2008

Supervised by

Docent Jussi Jero, MD, PhD
and
Docent Antti A. Aarnisalo, MD, PhD

Department of Otorhinolaryngology,
University of Helsinki and Helsinki University Central Hospital
Helsinki, Finland

Reviewed by

Docent Jyrki Törnwall, DDM, MD, PhD
Department of Oral and Maxillofacial Surgery,
University of Helsinki and Helsinki University Central Hospital
Helsinki, Finland

and

Docent Juha-Pekka Vasama, MD, PhD
Department of Otorhinolaryngology,
University of Tampere and Tampere University Central Hospital
Tampere, Finland

Discussed with

Professor Heikki Löppönen
Department of Otorhinolaryngology
University of Kuopio and Kuopio University Central Hospital
Kuopio, Finland

To my family

CONTENTS

ORIGINAL PUBLICATIONS

The thesis is based on the following original publications referred to in the text by their Roman numerals.

I Kinnari TJ, Peltonen LI, Kuusela P, Kivilahti J, Könönen M, Jero J. Bacterial adherence to titanium surface coated with human serum albumin. Otology & Neurotology 26: 380-384, 2005.

II Peltonen LI, Kinnari TJ, Aarnisalo AA, Kuusela P, Jero J. Comparison of bacterial adherence to polylactides, silicone, and titanium. Acta Oto-Laryngologica 127: 587-593, 2007.

III Peltonen LI, Jero J, Sukura A, Pietola L, Konttinen YT, Aarnisalo AA. Biocompatibility of polylactides in the middle ear: an experimental animal study. Otology & Neurotology 28: 850-853, 2007.

IV Peltonen LI, Aarnisalo AA, Kortesniemi MK, Suomalainen A, Jero J, Robinson S. Limited cone-beam computed tomography imaging of the middle ear: a comparison with multislice helical computed tomography. Acta Radiologica 48: 207-212, 2007.

V Peltonen LI, Aarnisalo AA, Käser Y, Kortesniemi MK, Robinson S, Suomalainen A, Jero J. Cone-beam CT: a new method for the imaging of the temporal bone. Submitted.

Publication **I** appears in Teemu Kinnari´s PhD thesis *"The effect of albumin coating on properties of tympanostomy tubes"*, and it has been published as part of this thesis with the permission of Dr. Kinnari and the Medical Faculty of the University of Helsinki.

ABBREVIATIONS

CBCT	cone-beam computed tomography
CFU	colony-forming unit
CMF	craniomaxillofacial
CNR	contrast-to-noise ratio
COM	chronic otitis media
CSOM	chronic suppurative otitis media
CT	computed tomography
CWD	canal wall down
CWU	canal wall up
DSA	digital subtraction angiography
EAC	external auditory canal
ET	Eustachian tube
FOV	field of view
HSA	human serum albumin
MRI	magnetic resonance imaging
PBS	phosphate-buffered saline
PGA	polyglycolic acid
PLA	polylactic acid
PLGA	polylactic-glycolic acid
PMMA	polymethylmethacrylate
PORP	partial ossicular replacement prosthesis
ROI	region of interest
RT	room temperature
TM	tympanic membrane
TORP	total ossicular replacement prosthesis
3D	three-dimensional

ABSTRACT

In the field of ear surgery, research continues on new applications for surgical reconstruction. Polylactic- and polyglycolic acid (PLA and PGA)-based degradable biomaterials are in wide clinical use especially in orthopedic and craniomaxillofacial (CMF) surgery, and in general they have proved to be safe and well-tolerated implant materials. Thus far, they have not been used in reconstructive human middle ear surgery. Common problems related to implant surgery are microbial biofilm formation on medical implants in vivo and subsequent infection. A postoperative implant infection often leads to re-operation and implant removal. The present thesis clarifies the surface properties of polylactic-glycolic acid (PLGA) in relation to bacterial adherence—the first step in biofilm formation—and the biocompatibility of the material in the middle ear. Furthermore, a new application has been studied for imaging of the middle ear with a lower radiation dose than with the present computed tomography (CT) of the ear. This method, cone-beam computed tomography (CBCT), has been used particularly in dental and maxillofacial imaging, where it allows accurate, three-dimensional (3D) imaging of a defined area.

The first two studies of this thesis tested bacterial adherence onto the surfaces of PLGA and of two common implant materials used in ear surgery: silicone and titanium. In the first study (I), a method was developed for quantifying in vitro adherence of two common pathogens of a chronically or postoperatively infected ear, *Staphylococcus aureus* and *Pseudomonas aeruginosa*, to the material surfaces, and for measuring the effect on adherence of a surface albumin coating. This method was utilized in the second work (II), where the adherence of these bacteria to PLGA, silicone, and titanium was studied and compared. In addition, the effect of albumin coating on adherence to these materials was tested and compared. Next, applicability of the PLGA material to reconstructive middle ear surgery was explored by study of its biocompatibility in the middle ear in an animal model (III) in which chinchillas were operated on, followed-up, and killed at 6 months postoperatively. In the experimental surgery, two kinds of PLGA implants were inserted into each animals' middle ear. Biocompatibilities of the implanted materials were evaluated according to clinical and

histological findings. Suitability of the CBCT for imaging of the ear was tested by imaging human cadaver temporal bones and comparing scaled accuracies of the images created by CBCT with those constructed with traditional multislice helical CT (IV). In addition, to evaluate the clinical applicability of CBCT to otologic diagnostics, a study was conducted of CBCT imaging of middle ear implants and operated temporal bones (V).

There proved to be no more bacterial adherence in vitro to the PLGA materials tested than to silicone and titanium. Of the materials studied, uncoated titanium clearly gathered the most bacteria, whereas differences in adherence levels between albumin-coated materials were smaller. Albumin coating significantly reduced bacterial adherence to every material tested. The biocompatibility of PLGA in the middle ear of the chinchilla was very good. In histological samples, only a mild inflammatory reaction was evident around the degrading PLGA plates. Clinically, no infections or extrusion of the implanted material occurred in the animals' external auditory canal (EAC) or middle ear. Limited cone-beam CT was found to be at least as accurate as conventional multislice helical CT in showing the clinically and surgically important landmarks of the middle and inner ear. The effective radiation dose was essentially lower with the CBCT than with the helical CT used in this study. Visualization of the middle ear structures and implants of operated temporal bones was clear and of diagnostic value.

Based on the results of Studies I to III, it can be concluded that PLGA is a safe and well-tolerated implant material in the middle ear area, and there is no greater in vitro adherence of *S. aureus* and *P. aeruginosa* to PLGA surfaces than to titanium and silicone. In addition, coating of these materials with albumin means that adherence of the bacteria to their surfaces can be substantially reduced, suggesting that this method may be useful in implant surgery as a preventive maneuver against postoperative infections. Based on the findings of Studies IV and V, cone-beam CT seems to be a promising new method for imaging the structures of the temporal bone. The diagnostic accuracy of CBCT corresponds to that of helical CT, while the radiation dose to patient per investigation remains lower with CBCT. Focused imaging with the lesser radiation exposure expands the possibilities for imaging the ear, especially when follow-up and limited uni- or bilateral examination is needed.

TIIVISTELMÄ (FINNISH SUMMARY)

Välikorvaleikkauksiin usein liittyvä välikorvan ja kuuloluuketjun kirurginen rekonstruktio on tapauskohtainen ja haasteellinen. Rekonstruktion tavoitteena on luoda olosuhteet, jotka mahdollistavat hyvän kuulon sekä välikorvan säilymisen tulehduksettomana ja ilmapitoisena. Kroonisesti tulehtunut välikorva aiheuttaa johtumistyyppisen kuulonaleneman ja lisää mm. kolesteatooman eli ”helmiäiskasvaimen” kehittymisen riskiä. Välikorvan kirurgisessa rekonstruktiossa on käytetty implanttimateriaaleina perinteisesti potilaan omia kudoksia, luuta, rustoa ja lihaskalvoa, sekä tarvittaessa erilaisia hajoamattomia biomateriaaleja. Uusia tekniikoita ja rekonstruktiivisia biomateriaaleja kokeillaan ja kehitetään jatkuvasti. Ongelmana biomateriaalien käytössä voi olla bakteerien adherenssi eli tarttuminen vieraan materiaalin pintaan, mikä saattaa johtaa biofilmin muodostumiseen. Tämä voi aiheuttaa kroonisen, huonosti antibiootteihin reagoivan infektion kudoksessa, mikä usein käytännössä johtaa uusintaleikkaukseen ja implantin poistoon.

Maitohappo- ja glykolihappopohjaiset biologisesti hajoavat polymeerit ovat olleet kliinisessä käytössä istutteina jo vuosikymmeniä. Niitä on käytetty erityisesti osteosynteesimateriaaleina ortopediassa sekä kasvo- ja leukakirurgiassa ja hyödynnetty myös urologiassa ja verisuonikirurgiassa stenttimateriaaleina. Niitä ei ole toistaiseksi käytetty välikorvakirurgiassa. Tässä väitöskirjassa on selvitetty polylaktaatti-glykolaattien (PLGA) bakteeriadherenssia in vitro suhteessa kahden yleisen korvakirurgisen implanttimateriaalin, titaanin ja silikonin bakteeriadherenssiin. Lisäksi on tutkittu eläinkoemallissa PLGA:n biokompatibiliteettia välikorvassa.

Korvan kuvantamiseen käytetään ensisijaisesti tietokonetomografiaa (TT), koska sen avulla saadaan tarkkaa tietoa korvan luisista ja ilmapitoisista rakenteista. TT-tutkimuksen ongelmana on potilaan altistuminen suhteellisen korkealle sädeannokselle, joka kasvaa kumulatiivisesti, jos kuvaus joudutaan toistamaan. Väitöskirjatyö selvittää uuden, aiemmin kliinisessä työssä rutiinisti lähinnä hampaiston ja kasvojen alueen kuvantamiseen käytetyn rajoitetun kartiokeila-TT:n soveltuvuutta korvan alueen kuvantamiseen. Kyseinen tekniikka

mahdollistaa tarkan kolmiulotteisen kuvantamisen rajatulta alueelta suhteellisen pienellä sädeannoksella.

Väitöskirjan kahdessa ensimmäisessä osatyössä tutkittiin ja verrattiin kahden kroonisia ja postoperatiivisia korvainfektioita aiheuttavan bakteerin, *Staphylococcus aureuksen* ja *Pseudomonas aeruginosan*, adherenssia titaanin, silikonin ja kahden eri PLGA-materiaalin pintaan in vitro. Lisäksi tutkittiin materiaalien albumiinipinnoituksen vaikutusta bakteeriadherenssiin. Ensimmäisessä, tutkimusmetodeihin keskittyvässä osatyössä tutkittiin bakteeriadherenssia titaanilevyillä. Menetelmää hyödynnettiin edelleen toisessa osatyössä, jossa tutkittiin ja vertailtiin bakteerien adherenssia myös muihin biomateriaaleihin. Kolmannessa osatyössä tutkittiin eläinmallissa PLGA:n biokompatibiliteettia kokeellisessa välikorvakirurgiassa. Chinchillojen välikorviin istutettiin PLGA-materiaalia, eläimiä seurattiin, ja ne lopetettiin 6 kk:n kuluttua operaatiosta. Biokompatibiliteetin arviointi perustui kliinisiin havaintoihin sekä kudosnäytteisiin. Neljännessä osatyössä tutkittiin kartiokeila-TT:n soveltuvuutta korvan alueen kuvantamiseen vertaamalla sen tarkkuutta perinteisen spiraali-TT:n tarkkuuteen. Molemmilla laitteilla kuvattiin kadavereista preparoituja ohimo- eli temporaaliluita korvan alueen kliinisesti ja kirurgisesti tärkeiden rakenteiden kuvantumisen tarkkuuden arvioimiseksi. Viidennessä osatyössä arvioitiin myös operoitujen temporaaliluiden ja välikorvaimplanttien kuvantumista kartiokeila-TT:ssa.

Bakteeriadherenssitutkimuksissa osoittautui, että PLGA-materiaalin pintaan tarttui keskimäärin korkeintaan saman verran tai vähemmän bakteereita kuin silikonin. Pinnoittamaton titaanilevy keräsi bakteereita eniten. Albumiinipinnoitus vähensi bakteeriadherenssia merkitsevästi kaikilla materiaaleilla. Eläinkokeiden perusteella PLGA todettiin hyvin siedetyksi välikorvassa. Korvakäytävissä tai välikorvissa ei todettu infektioita, tärykalvon perforaatioita tai materiaalin esiin työntymistä. Kudosnäytteissä näkyi vain lievää tulehdusreaktiota ja fibriinin muodostumista implantin ympärillä. Temporaaliluutöissä rajoitettu kartiokeila-TT todettiin vähintään yhtä tarkaksi menetelmäksi kuin spiraali-TT välikorvan ja sisäkorvan rakenteiden kuvantamisessa, ja sen aiheuttama kertasäderasitus todettiin spiraali-TT:n vastaavaa selvästi vähäisemmäksi. Kartiokeila-TT soveltui hyvin välikorvaimplanttien ja postoperatiivisen korvan kuvantamiseen.

Osatöiden I-III perusteella voidaan todeta, että PLGA on välikorvakirurgiaan soveltuva, turvallinen ja kudosyhteensopiva biomateriaali. PLGA ei adheroi bakteereja in vitro enempää

kuin välikorvakirurgiassa implanttimateriaaleina jo pitkään käytetyt titaani tai silikoni. Kaikkien osatöissä testattujen biomateriaalien pinnoittaminen albumiinilla vähentää bakteerien adherenssia niihin merkittävästi, mikä puoltaa pinnoituksen käyttöä implanttikirurgiassa. Osatyöt IV ja V osoittavat, että kartiokeila-TT soveltuu korvan alueen kuvantamiseen. Sen tarkkuus kliinisesti tärkeiden rakenteiden osoittamisessa on vähintään samaa luokkaa kuin spiraali-TT:n. Yhden rajoitetun kartiokeila-TT-tutkimuksen potilaalle aiheuttama sädeannos on pienempi kuin nykyisen rutiinikäytössä olevan korva-spiraali-TT:n. Tämä tekee menetelmästä potilasturvallisemman vaihtoehdon spiraali-TT:lle erityisesti, jos potilaan tilanne vaatii seurantaa ja useampia kuvauksia, ja jos halutaan kuvata rajoitettuja alueita uni- tai bilateraalisesti.

1
INTRODUCTION

Reconstruction in middle ear surgery is challenging in many ways. The ear surgeon has to create favorable circumstances for the healing process to ensure an aerated tympanum and the satisfactory hearing of the patient in the long term. To reach these goals, use of implant materials is often mandatory. Traditionally, the patient's own bone, cartilage, and fascia have been used as grafting material. In addition, various kinds of biomaterials have shown variable success. Especially in radical operations, where lack of sufficient reconstruction material and structural support may constitute a problem, but also in other ear surgery as well, new, better operative techniques are desirable.

Polylactic-acid (PLA)- and polyglycolic acid (PGA)-based biodegradable copolymers have long been used in orthopedic and craniomaxillofacial (CMF) surgery as osteosynthesis materials (Törmälä et al. 1998, Suuronen et al. 2000, Waris et al. 2004). They have also served as urethral stent material (Tammela and Talja 2003), and during the past 10 years, further applications have been under intensive research with promising results (e.g. tracheal and drug-releasing vascular stents made of polylactide frame) (Korpela et al. 1999, Hietala et al. 2001, Nalwa et al. 2001, Vogt et al. 2004). In clinical use, these polymers have proven safe implant materials with low complication rates. Thus far, they have not been routinely used in human middle-ear surgery, and only some experimental data exist about their applicability to myringoplasty (Feenstra et al. 1984), to drug-delivery in the middle ear (Goycoolea et al. 1991, 1992, 1994), or to tympanostomy tubes (Massey et al. 2004).

Every medical implant has the potential to become covered with microbial biofilm, a major cause of resistant postoperative infections (An and Friedman 1998, Lynch and Robertson 2008). It is therefore desirable to find implant materials with surface characteristics unfavorable for bacterial adhesion and biofilm formation. Furthermore, different kinds of methods that could inhibit bacterial adherence onto the implant surface are under continuous development and research. In developing such a process, one of the goals is to make it easily applicable to clinical use. Coating of any material with human serum albumin (HSA)—a

method known for four decades (Packham et al. 1969)—is a relatively simple way to convert the material surface so it becomes less susceptible to bacterial adhesion. Albumin coating has been applied in research into implant surgery in the past two decades (Zdanowski et al. 1993, An et al. 1996 and 1997), and it has also been used to prevent platelet adhesion in extracorporeal hemoperfusion systems and vascular surgery (Remuzzi and Boccardo 1993, al-Khaffaf and Charlesworth 1996).

Radiological imaging of the ear is often required in planning surgical therapy of the middle ear or when follow-up of the disease—with or without operative treatment—is necessary. Computed tomography (CT) is basically the method of choice when imaging the ear because of the need for accurate visualization of the thin bony structures and air-filled spaces. Other imaging techniques with more specific indications, mainly magnetic resonance imaging (MRI), are complementary and sometimes also needed (Kösling and Bootz 2001, Maroldi et al. 2001, Williams and Ayache 2004). The significant disadvantage of the conventional multislice helical CT, however, is the relatively high radiation dose per investigation to which the patient is exposed. Furthermore, the dose increases cumulatively when repeated investigations are needed, as sometimes may be the case during follow-up. Clinical cone-beam computed tomography (CBCT) is a relatively new imaging method developed for diagnostic three-dimensional (3D) imaging of dental and facial areas (Arai et al. 1999, Sukovic 2003). This technique is under ongoing development, and it has already been used for research and clinical purposes to image other objects as well (Robinson et al. 2005). One of the advantages of the CBCT, when compared with conventional helical CT, is its lower radiation dose per investigation when focusing the imaging on a limited field, e.g., unilaterally or on the diseased area only. This aspect does raise the question whether CBCT could be an alternative to helical CT in imaging the ear, in particular when repeated information from a relatively limited area is required.

The purpose of this study was to investigate the bacterial adherence to polylactic-glycolic acid (PLGA) in comparison to common otologic implant materials, to test the effect of albumin coating on such adherence, to clarify the biocompatibility of PLGA in the middle ear, and to explore the suitability of CBCT to otologic imaging.

2
REVIEW OF THE LITERATURE

2.1 CHRONIC OTITIS MEDIA AND CHOLESTEATOMA

2.1.1 Definitions

Chronic suppurative otitis media (CSOM) involves chronic inflammation of the middle ear and the mastoid mucosa. In addition, a nonintact tympanic membrane (TM) (perforation or tympanostomy tube) and otorrhea are present (Bluestone and Klein 1995). Adhesive otitis media involves permanent atelectasis and retraction of the TM such that the middle ear space is totally obliterated. No mucosal surfaces are present, since the TM is adherent to the auditory ossicles and promontory (Cummings et al. 1998). Chronic otitis media (COM) includes both adhesive and suppurative otitis media.

Cholesteatoma is a non-neoplastic lesion consisting of keratinizing stratified squamous epithelium and desquamating epithelium of keratin within the middle ear or other pneumatized portions of the temporal bone. Cholesteatoma can be congenital or acquired; in the latter case it is associated with COM and related conditions (Bluestone and Klein 1995, Persaud et al. 2007).

2.1.2 Epidemiology

Chronic suppurative otitis media most often occurs in the first 5 years of life. Furthermore, it is most common in developing countries, in special populations (e.g., in children with craniofacial anomalies), and in certain racial groups. Prevalences of CSOM in children range from less than 1% up to 46% worldwide, being lowest in highly developed countries (Verhoeff et al. 2006). Adhesive otitis media may develop as a result of long-lasting chronic middle ear infection in a small percentage of the patients (Bluestone and Klein 1995, Cummings et al. 1998).

The prevalence of cholesteatomas is unknown, and the incidence of all cholesteatomas has been estimated at 3 to 6 per 100 000 (Kazahaya and Potsic 2004). In a histopathological study of 144 temporal bones showing chronic otitis media (da Costa et al. 1992), cholesteatoma was found in 36% of the temporal bones with a perforated TM, and in 4% of the bones without. Congenital cholesteatoma is a rarity, accounting for 4 to 24% of cholesteatomas in children and 2 to 5% of all cholesteatomas (Kazahaya and Potsic 2004, Lazard et al. 2007).

2.1.3 Etiology and pathogenesis

Several identified risk factors exist for development of CSOM, including a history of acute and recurrent otitis media, parental history of otitis media, and large day-care groups. The pathogenesis of CSOM is multifactorial, and both environmental and genetic factors contribute to the likelihood of the disease. In addition, pathology in the anatomy and physiology of the Eustachian tube (ET) is involved (Bluestone and Klein 1995, Seibert and Danner 2006, Verhoeff et al. 2006). Bacteria isolated in CSOM are most typically *Pseudomonas aeruginosa*, *Staphylococcus aureus*, *Proteus spp.* among the aerobes, and *Bacteroides spp.* among the anaerobes (Kenna et al. 1986, Fliss et al. 1990, 1992, Arguedas et al. 1994, Indudharan et al. 1999, Aslam et al. 2004). They can enter the middle ear either through the ET or from the external auditory canal (EAC) through a nonintact TM. Fungi may also be present. It is still unclear whether the bacteria play a role in the CSOM development or represent secondary contamination in the inflamed middle ear (Brook 1995). With growing evidence for bacterial biofilms' being a major cause of resistant, chronic infections on tissue or implant surfaces (Costerton et al. 1999, Stewart and Costerton 2001), the existence of these biofilms in CSOM and infected cholesteatomas has become obvious (Post 2001, Chole and Faddis 2002, Hall-Stoodley et al. 2006). The eventual role of the biofilms in these diseases is under investigation and is yet to be clarified.

Several hypothetical mechanisms for the pathogenesis of acquired cholesteatoma exist. Dysfunction of the ET has been assumed to be an important factor for development of a retraction pocket of the TM (Chao et al. 1996, Seibert and Danner 2006). ET dysfunction leads to negative pressure in the middle ear cavity, which first causes retraction and invagination of the TM, usually in its most elastic pars flaccida area, but may involve the whole TM as well (Palva 1990, Ramakrishnan 2007). Gradually, the pocket becomes filled with keratin and debris to form a continually expanding cholesteatoma (Semaan and Megerian

2006). Migration of the skin epithelial cells of the EAC over the TM perforation edges to the middle ear is another proposed mechanism, as well as basal cell invasion in the middle ear behind an intact TM (Palva 1990). There also exists some evidence for potential keratinization of the middle ear mucosa through metaplasia in vitamin A-deficient animals (Chole 1979), but this mechanism still remains highly controversial in the literature (Persaud et al. 2007). Recent findings suggest that apoptosis plays an important role in the pathogenesis of cholesteatoma; it also seems to participate in the differentiation and accumulation of keratin debris and expanding of cholesteatoma (Olszewska et al. 2006). The presence of CSOM or adhesive otitis media with or without TM perforation predisposes to the development of cholesteatoma (Bluestone and Klein 1995), as do traumatic or iatrogenic perforations of the TM (Buckingham 1981, Al Anazy 2006, Persaud et al. 2007).

The cause of congenital cholesteatoma remains somewhat controversial, as well. The two main hypotheses are the epithelial rest and invasion theories (Kazahaya and Potsic 2004). Findings of epithelial rests in the anterosuperior quadrant of the middle ear, and DNA differences found between acquired and congenital cholesteatoma support the epithelial rest theory (Karmody et al. 1998, Kojima et al. 2001), whereas evidence for the invasion theory suggests a misdirection of migrating ectodermal cells from the developing EAC (Aimi 1983, Kazahaya and Potsic 2004). The original criteria for congenital cholesteatoma were the presence of a white “pearl” behind an intact TM without history of perforation, otorrhea, and otologic surgery, but later, a history of acute otitis media, otitis media with effusion, and otorrhea have also been included (Koltai et al. 2002, Nelson et al. 2002).

2.1.4 Clinical course

COM leads to a conductive and—in some cases also sensorineural—hearing loss in that ear. Furthermore, chronic inflammation and infection can corrode the mucosa and bony structures of the middle ear and contribute to the formation of a middle ear cholesteatoma (Bluestone and Klein 1995, Cummings et al. 1998). In CSOM, otorrhea through a perforated TM is often present, and otalgia may occur. Labyrinthitis as a consquence of chronic middle ear infection is possible, and more rarely, serious complications, such as acute mastoiditis, petrositis, sinus thrombosis, or intracranial infections occur (Leskinen and Jero 2005, Hafidh et al. 2006, Smith and Danner 2006). In adhesive otitis media, aeration of the middle ear is prevented by

obstruction or dysfunction of the ET, which leads to retraction of the TM, collapse of the tympanum, and conductive hearing loss of varying degrees (Bluestone and Klein 1995).

A prograding middle ear cholesteatoma causes hearing loss (either conductive or combined), destroys its surrounding structures, and may, if not treated, invade the petrosal part of the temporal bone, facial canal, and intracranial space. Consequently, petrositis, paresis of the facial nerve or other cranial nerves, intracranial infection, or trauma to the intracranial structures may follow. A labyrinthine- or cerebrospinal fluid fistula may also develop (Cummings et al. 1998, Kazuharu et al. 2005, Smith and Danner 2006).

2.1.5 Diagnosis and treatment

Diagnosis of COM is based on the clinical picture. Disease severity can be assessed by audiograms, sonotubometry, and radiological examinations (mainly CT). In CSOM, bacterial culture of middle ear secretion is a good diagnostic tool when planning treatment with antibiotics. CSOM is relatively resistant to nonsurgical treatment, but oral as well as topical antibiotics may be useful. The best response to otorrhea has been with the use of topical antibiotics (Verhoeff et al. 2006). However, medication often provides only temporary relief of symptoms. Surgical treatment of COM consists of tympanomastoidectomy followed by reconstruction of the middle ear (Bluestone and Klein 1995, Brackmann et al. 2001). The decision for surgical treatment has to be based on careful evaluation of each patient's individual situation. Youth, good overall health, or systemic diseases requiring careful elimination of infectious foci favor surgery, whereas risk factors for operative treatment and anesthesia such as high age and certain diseases speak in favor of follow-up and conservative care.

Diagnostic guidelines for cholesteatoma are similar to those for COM. Clinical examination of the ear is most important with suspected cholesteatoma based on patient's history and symptoms (history of COM, hearing loss, otalgia, otorrhea). Cholesteatoma may long remain asymptomatic. Intensive retraction of the pars flaccida and a white mass visible in perforation of the TM or in the middle ear through an intact TM are signs pathognomonic of cholesteatoma (Palva 1990, Bluestone and Klein 1995). Sometimes it is necessary to first treat the overlying infection in order to examine the ear properly. The ultimate diagnosis may also remain to be defined during surgery. Imaging of the ear with CT provides valuable

information on extent of the disease and helps with treatment planning (Maroldi et al. 2001). MRI is sometimes needed for differential diagnostics, for instance, for to distinguish cholesteatoma from cholesterol granuloma (Kösling and Bootz 2001, Williams and Ayache 2004). Treatment of the cholesteatoma is in most cases surgical. Radical surgery and a long postoperative follow-up are usually mandatory. High age and other risk factors for anesthesia or surgery, combined with rather limited disease, argue for conservative treatment.

2.2 SURGICAL TREATMENT OF CHRONIC OTITIS MEDIA AND CHOLESTEATOMA

2.2.1 Surgical approach and eradication of the disease

In the case of CSOM, a tympanomastoidectomy is first performed, which gives the surgeon a direct view of the mastoid and middle ear. During the tympanomastoidectomy, all the diseased bone and mucosa in the mastoid area are removed. Thereafter, the inflamed mucosa and debris in the middle ear are carefully stripped away (Cruz et al. 2003). Finally, reconstruction of the tympanic cavity, the auditory ossicular chain, and the TM will take place to the extent needed (Hüttenbrink 1994, Brackmann et al. 2001). Adhesive otitis media is a surgically difficult disease entity. Several different tympanoplasty techniques have been described to restore an air-filled and functional tympanic cavity, most of them using cartilage chips as reconstruction material (Hüttenbrink 1994). However, if the ET is permanently obstructed and dysfunctional, the results of surgical treatment attempts are often poor.

The surgical approach to a cholesteatoma depends on the size and location of the diseased area. With small, epitympanic cholesteatomas, a transcanal atticotomy may be sufficient to eradicate the disease if it provides a direct, good visualization of the operative field (Palva 1993). In atticotomy, an endaural incision is made, a tympanomeatal flap is formed, and sufficient bone between the EAC and the epitympanum (atticus) is drilled away to visualize the cholesteatoma. Subsequently, the cholesteatoma and all the diseased tissue is dissected from the epitympanum and removed, the epitympanic bony defect is reconstructed with cartilage or bone, and the tympanomeatal flap is repositioned. Reconstruction of the TM is executed when necessary (Palva 1987b, Brackmann et al. 2001).

With larger cholesteatomas extending towards the hypotympanum or medially, a canal wall-up (CWU) or canal wall-down (CWD) tympanomastoidectomy is required to reach and visualize the whole diseased area (Palva 1993). With the CWD technique, the entire posterior bony wall of the EAC is removed, resulting—if reconstruction of the wall will not be performed (radical operation)—in an open cavity postoperatively. In the modified radical operation, the posterior wall will be reconstructed (Black 1998, Mukherjee et al. 2004).

With the CWU technique, the posterior wall will not be removed, and the approach to the middle ear may or may not involve the facial recess (Brackmann et al. 2001). After removal of the cholesteatoma, the tympanic cavity, the auditory ossicular chain, and the TM can be reconstructed either primarily or later in the second-look operation (Kim et al. 2006). The advantages and disadvantages of the CWD- and CWU techniques are in Table 1. The choice between these techniques can be made either preoperatively or intraoperatively.

2.2.2 Reconstruction

After removal of diseased tissue from the middle ear, reconstruction of the auditory ossicular chain is often essential for maintenance or improvement of hearing. It is equally important to be able to reconstruct the tympanic cavity and the level of the TM in such a way that the tympanum will not totally collapse over time, which in turn would result in adhesive otitis media, conductive hearing loss, and increasing risk for a recidive cholesteatoma (Cummings et al. 1998, Brackmann et al. 2001). In cholesteatoma surgery, the reconstruction may be left to the second-look operation. Furthermore, obliteration of the radical cavity (Palva 1979), reconstruction of the posterior wall of the EAC, and meatoplasty after a CWD operation are usually added to the final procedure, if needed.

In surgery for CSOM, removal of the inflamed mucosa and of possible granulation or polyps of the middle ear followed by myringoplasty may be sufficient, if the auditory ossicular chain is intact. In the case of a disrupted, partially absent, or ossified chain, the chain must undergo reconstruction. Autologous bony grafts are recommended as the approach, but lack of appropriate reconstruction material may become a problem. If no autograft columella is available, biomaterial implants are an option (Brackmann et al. 2001).

In cholestetoma surgery, the challenges of reconstruction increase in proportion to the radicality of the operation (Table 1). On the other hand, a second-look operation is sometimes needed after CWU, which in turn is not usually the case after CWD. If the destruction in the middle ear caused by the cholesteatoma has been extensive, the procedure of choice is CWD (Palva 1990). Reconstruction of the tympanum after CWD is difficult and—even if successful—results in minitympanum and poorer hearing than after CWU (Palva 1987a). The ossicular chain is most often corroded by cholesteatoma and therefore partly or in some cases even totally absent and has to be reconstructed. Again, autologous grafts are used initially (Palva 1990), but biomaterials also serve (Brackmann et al. 2001). If the radical cavity will be obliterated and the posterior wall of the EAC reconstructed, reconstruction material may be insufficient (bone chips and paté; Palva 1993), especially if most of the bone tissue drilled away was diseased. The advantages of the reconstructed posterior wall—compared to an open radical cavity—are the better circumstances for cleaning and examination of the cavity during the postoperative follow-up in addition to avoidance of meatoplasty (Takahashi et al. 2007). Use of the musculoperiosteal flap (Palva´s flap) supports the reconstructed and obliterated wall (Palva and Mäkinen 1979) and, in the case of radical cavity, makes the cavity easier to clean postoperatively.

2.2.3 Implant materials

In reconstruction of the auditory ossicular chain and the TM, autografts are usual, if available (Palva 1987b, Brackmann et al. 2001). The primary goal is to remodify the incus to create a short or a long columella, depending on the clinical status of the stapes. In the former, the remodified incus will be placed between the malleus and stapes head, in the latter case, between the malleus and stapes footplate. If the remnants of the incus cannot be utilized, cortical bone with tragal cartilage (against the tympanic membrane) can serve, especially in cholesteatoma surgery, where disease may have destroyed or contaminated the whole ossicular chain. Reconstruction of the TM requires mostly autologous fascia or cartilage (Palva 1987b, Brackmann et al. 2001).

If the malleus is intact, but the incus is not usable, several biomaterials are available. The longest used implant material with excellent biocompatibility, hydroxyapatite, has been in use since the early 1960s with good results (Grote 1990 and 1998, Brackmann et al. 2001). In the development of hydroxyapatite prostheses, a milestone in 1996 was introduction of the

HAPEX prosthesis. In this application, a hydroxyapatite-reinforced polyethylene composite cuff or shaft is attached to the dense hydroxyapatite body, allowing the surgeon to intraoperatively adjust the length and shape of the prosthesis more easily than those of a prosthesis made of pure hydroxyapatite (Brackmann et al. 2001).

Alternatively, a titanium partial ossicular replacement prosthesis (PORP) or a total ossicular replacement prosthesis (TORP) with a cartilage graft is an adequate choice (Neumann et al. 2003, Fisch et al. 2004, Truy et al. 2007). The broad base of a PORP or a TORP contacts the TM or malleus handle (via the cartilage graft) and extends either to the head of the stapes (PORP) or directly to the footplate (TORP), replacing part of the ossicular chain. Titanium prostheses have proven safe and stabile implants with low complication rates and good hearing results (Dalchow et al. 2001, Fisch et al. 2004).

When reconstructing the posterior wall of the EAC and obliterating the radical cavity, use of bone (chips and paté) and fascia is advisable (Palva 1993). Furthermore, the radical mastoid cavity can be partially filled with and the reconstruction supported posteriorly by a musculoperiosteal flap (Palva and Mäkinen 1979). In the case of a large cavity or lack of bone paté, porous hydroxylapatite ceramic may be one option (van Blitterswijk and Grote 1990, Grote 1998, Takahashi et al. 2007). The decision as to reconstruction and implant materials is based on the clinical situation, on intraoperative findings, and on the patient's individual needs (Black 1998, Cummings et al. 1998, Brackmann et al. 2001).

Table 1. Advantages and disadvantages with canal wall up (CWU) and canal wall down (CWD) procedures (Palva 1987a and 1993, Cummings et al. 1998, Brackmann et al. 2001).

	Advantages	**Disadvantages**
CWU	- level of tympanic membrane easier to reconstruct - postoperatively aerated tympanum more likely achievable - absence of problems caused by excavation of radical cavity	- residual / recurrent cholesteatomas more likely (25%) - problems with surgical control over facial recess and sinus tympani - second-look operation sometimes necessary
CWD	- residual or recurrent cholesteatoma easier to observe - recurrences rare (up to 10%) - surgical control of facial recess and sinus tympani areas	- minitympanum postoperatively - problems with reconstruction - poorer hearing result - cavity-cleaning problems

2.3 MEDICAL BIOMATERIALS AND BACTERIAL ADHERENCE

2.3.1 Definitions and background

Biomaterials and medical implants made of biomaterials are synthetic or nature-derived products to be used in contact with tissue, blood, or tissue fluids for prosthetic, diagnostic, or therapeutic purposes. A medical implant must be used in such a way that it does not interfere with the vital functions of the host organism (Törmälä et al. 2003). Based on their chemical composition, biomaterials can be divided into metals, polymers, ceramics, composites, and materials of biological origin (Törmälä et al. 2003). The division can also be made according to the reactivity of the material surface: 1) almost inert materials with smooth surfaces, 2) almost inert materials with porous surfaces, 3) materials with chemically reactive surfaces, and 4) resorbable materials (Hench and Ethridge 1982, Gross and Strunz 1985).

Polymeric biomaterials can be divided into three groups: biostabile, bioabsorbable (biodegradable or resorbable), and partially biodegradable. Ideal biostabile polymers are physiologically inert, cause a minimal response in the host tissue, and maintain their qualities for years or decades in vivo, whereas resorbable materials will be gradually degraded by the activity of the host tissue and by purely physicochemical reactions (Törmälä et al. 1998). Biodegradable materials are the best alternative in situations requiring temporary implant treatment. The main demand for a resorbable material and its degradation products is good biocompatibility. Furthermore, in the beginning of the healing process they should retain the tissue fixation required, and during degradation, all mechanical stress should gradually be shifted to the healing tissue. If no serious complications occur, such as resistant postoperative infection, no need will arise for a removal operation. Furthermore, after complete resorption, the risk for complications is considerably diminished (Törmälä et al. 1998).

Most biomaterials cause non-specific tissue reactions around the implant. In clinical medicine this phenomenon is to some extent acceptable—sometimes even desirable (Ratner 1993). Biocompatibility is the term to describe the likelihood of a material to induce a non-specific tissue response in a biological environment, e.g., inflammatory and foreign body reactions (Williams 1989, Ratner 1993); in the case of poor biocompatibility, these reactions are severe. Furthermore, bacterial adhesion to a biomaterial may cause a biomaterial-centered infection leading to poor tissue integration or poor compatibility of the implant (Gristina 1987). A biomaterial with good biocompatibility induces at most a mild reaction. If the reaction results in fibrosis, the implant material is classified as biotolerant. In in vivo conditions, a material may form a direct bond to the bone or cartilage; then it is called bioinert (as with titanium). Some materials with chemically reactive surfaces can evoke a tissue response that leads to integration with bone (as with bioglass); these materials are called bioactive (Törmälä et al. 2003).

2.3.2 Biofilm formation

According to Costerton et al. (1995), “Biofilms are defined as matrix-enclosed bacterial populations adherent to each other and/or to surfaces or interfaces.” A biofilm consists of bacteria or fungi and their extracellular matrix, which together form a microenvironment that essentially differs from the environment of free microbes. Biofilm usually comprises many

species of microbes, but it can also comprise a single species (Costerton et al. 1999). Biofilm microbes do possess a phenotype, metabolism, and a division rate different from those of planktonic counterparts (Costerton et al. 1995, Lynch and Robertson 2008). Partly due to their reduced activity, biofilms are very resistant to antiobiotic treatment and to the host's immune system (Stewart and Costerton 2001, Lynch and Robertson 2008). Numerous activities maintain or strengthen the structure and function of these micro-ecosystems, such as interchange of plasmids between the bacteria. Recent studies have indicated that controlled death and lysis of bacterial cells also play an essential role in the formation and stability of the biofilm (Bayles 2007).

With regard to bacterial biofilms, adherence of bacteria to a surface is the first step in biofilm formation (van de Belt et al. 2001, Palmer et al. 2007). Thus, microbial adhesion to the surface of a medical implant may lead to biofilm formation and chronic infection, which in turn leads to increased postoperative morbidity and mortality, and often requires removal of the implant (van de Belt et al. 2001, Darouiche 2004, Kojic and Darouiche 2004, Pawlowski et al. 2005, Lynch and Robertson 2008). Furthermore, strong evidence exists for bacterial biofilms' being a major factor in some chronic implant-free infections in the head and neck area, such as CSOM (Hall-Stoodley et al. 2006, Post 2001), chronic tonsillitis (Chole and Faddis 2003, Post et al. 2004 and 2007) and rhinosinusitis (Sanclement et al. 2005), and infected cholesteatoma (Chole and Faddis 2002).

2.3.3 Implant surface characteristics with reference to bacterial adherence

The material-dependent factors that influence bacterial adhesion to a biomaterial surface are the chemical composition of the material, the charge and hydrophobicity of the surface, and the physical configuration and roughness of the surface. Metal and glass surfaces are negatively charged and hydrophilic, while polymers are less electrostatically charged and are hydrophobic (An and Friedman 1998). Surface roughness has been considered an important factor in bacterial adherence (van de Belt et al. 2001), with several attempts at explanations as to why bacteria prefer to adhere to rougher surfaces (Scheuerman et al. 1998), but the literature provides somewhat contradictory evidence, and it seems obvious that this topic as well as the influence of charge and hydrophobicity are complicated and not yet fully understood (Hogt et al. 1985, Verheyen et al. 1993, An and Friedman 1998, van de Belt et al. 2001, Emery et al. 2003, Katsikogianni and Missirlis 2004, Palmer et al. 2007). Evidence is,

however, strong that surfaces with irregularities and grooves promote more bacterial adhesion and biofilm formation than do smooth surfaces (McAllister et al. 1993, Quirynen et al. 1993, Verheyen et al. 1993, Scheuerman et al. 1998), presumably resulting from greater surface area and more sheltered sites for microbial colonization. The physical configuration of a material surface is a complicated 3-dimensional parameter related to surface ultrastructure and can be routinely evaluated by scanning electron microscopy (An and Friedman 1998); hence, it differs from surface roughness, which is simpler and detectable under light microscopy. Configuration indicates morphological description (for instance: a porous or a monofilament surface). The effect of physical configuration on bacterial adherence has been established for instance with dental materials, in which infection rates at the implant site have been much higher with porous than with dense implant materials (Merritt et al. 1979).

2.3.4 Bacterial adherence to biomaterial surfaces

In addition to these material-dependent factors influencing the bacterial adhesion process are environmental factors and bacterial properties unique to different species (An and Friedman 1998, van de Belt et al. 2001, Katsikogianni and Missirlis 2004). In general, the theory is that bacteria with hydrophobic properties prefer hydrophobic surfaces, and those with hydrophilic qualities prefer hydrophilic surfaces (An and Friedman 1998), but contradictory data and exceptions to this rule exist, as well (Chu and Williams 1984, Hogt et al. 1985, Verheyen et al. 1993, van de Belt et al. 2001, Karakeçili and Gümüşderelioğlu 2002, Emery et al. 2003).
Bacterial adhesion to surfaces and interfaces in vivo is, all in all, a very complicated process with numerous intervening factors. Their contribultion will depend, for instance, on the surrounding media, tissue-specific factors, bacterial concentration and flow, and temperature (Gristina 1987). Furthermore, unique surface characteristics and the behavior of differing bacterial species and strains do have their individual impact on adherence (An and Friedman 1998, Palmer et al. 2007). Concentration of antibiotics in the surrounding tissue and immunological mechanisms of the host also influence the adhesion (Gristina et al. 1985 and 1987, Lynch and Robertson 2008). After exposure to an in vivo environment, the implanted biomaterial becomes covered with proteins and other macromolecules within seconds, well before the appearance of the first micro-organisms. This adsorbed coverage, called “conditioning film,” can alter surface properties of the biomaterial to be more or less favorable to bacterial adhesion (van de Belt et al. 2001). In fact, the adhering microbes rarely attach to a pure biomaterial surface in vivo, but to this conditioning film. They can migrate to

the surface by various transport mechanisms such as diffusion, convection, or sedimentation (van de Belt et al. 2001, Palmer et al. 2007).

Initial bacterial adhesion to a substratum, according to one major theory, results from a combination of attractive Lifshitz-Van der Waals forces, attractive or repulsive acid-base interactions, and generally repulsive electrostatic interactions (van de Belt et al. 2001, Palmer et al. 2007). Consequently, some evidence suggests that the hydrophobicity of biomaterial surfaces determines which proteins will adsorb to the surface from the biological surroundings. Surface hydrophobicity would thus be one of the major factors to control bacterial adhesion to conditioning films. For example, hydrophobic biomaterials used in the human oral cavity and in the oropharynx have been found to gather more biofilm than do hydrophilic ones (Quirynen et al. 1988, Everaert et al. 1997). However, in some studies, surface hydrophobicity has little or no effect on bacterial adhesion (Karakeçili and Gümüşderelioğlu 2002, Palmer et al. 2007). The initial adhesion of bacteria is reversible. This reversible attachment may, however, turn irreversible through firm anchoring caused by production of exopolymers that can cover the biofilm to form a so-called "glycocalyx." This term indicates the assembling of glycoproteins onto the biomaterial (Gristina and Costerton 1985), and in addition to anchoring the biofilm, the glycocalyx protects the bacteria against antibiotics and host defence mechanisms (Brown et al. 1988, van de Belt et al. 2001, Palmer et al. 2007)

2.3.5 Prevention of bacterial adherence

For decades, a great amount of work has been devoted to exploring methods for preventing or reducing bacterial adherence to medical implants. Numerous procedures have emerged, and further research uses new technologies and materials. Coating the implant surface with substances of an anti-adherent nature or treating the surface with certain processes will considerably inhibit bacterial adhesion (von Eiff et al. 2005a, Qiu et al. 2007). Furthermore, implants can be impregnated with antimicrobial agents (Cormio et al. 1997, Multanen et al. 2000a, von Eiff et al. 2005b, Darouiche et al. 2007, Darouiche 2007), or biodegradable implants may release antibiotics during degradation (Niemelä et al. 2006). The material itself may also be selected for specific purposes based on its known anti-adhesive properties (von Eiff et al. 2005b). The aim of anti-adhesive methods is to change the surface characteristics of the biomaterial—mainly charge and hydrophobicity—in order to make it more undesirable for

bacteria to adhere to. Because of the complexity of the adhesion process, especially the species-dependent behavior, we have no exact rules or schemes that would be generally applicable to all materials and bacteria.

Ionizing of otologic implant material surfaces (fluoroplastic and silicone) has been effective in preventing bacterial adhesion and biofilm formation by *Staphylococci* and *Pseudomonas aeruginosa* in vitro (Biedlingmaier et al. 1998), and by *Staphylococcus aureus* in vivo (Saidi et al. 1999). Treating silicone tympanostomy tubes with silver oxide has reduced postoperative otorrhea (Chole and Hubbell 1995), but this method could not inhibit bacterial adherence in the study by Biedlingmaier et al. (1998), who concluded that ionized fluoroplastic was the most effective combination against bacterial adherence. Saidi et al. (1999) found no biofilm inhibition in vivo on silver oxide-impregnated tympanostomy tubes; in this setting, ion-implanted silicone was superior to non-treated and silver-oxide treated fluoroplastic tubes. Based on their results, this group also suggested that in prevention of persistent otorrhea, adherence characteristics of the tube material may be more important than antibacterial coatings. In short, bombarding of the tympanostomy tube surface with ions seems to be a relatively effective method for preventing or inhibiting bacterial adherence, whereas coating the surface with silver oxide provides somewhat contradictory results. On the other hand, Lundeberg (1986) showed a decrease in catheter-associated urinary tract infections with silver oxide-coated catheters. Multanen et al. (2000b) found that coating PLA urological stents with silver nitrate prevented bacterial adherence to the stents in vitro; the effect was tested with uropathogenic bacteria, including *Pseudomonas aeruginosa*.

2.3.6 Albumin coating

Serum or tissue proteins are known to have interactions with bacteria and an influence on bacterial adhesion, for instance to biomaterials, in either binding to the material surface or to a bacterial surface, or in being present in the liquid medium during the adhesion process (An and Friedman 1998). These proteins can enhance or inhibit bacterial adhesion, depending on the protein itself and the binding target (material surface, bacterial surface, or both), and they also may act as mediators in the binding process between bacteria and surfaces (Kuusela et al. 1985, Cunliffe et al. 1999, Štyriak et al. 1999). The bacteria and proteins bind to each other mostly with specific ligand- and receptorlike interactions, and the proteins may change the chemical properties of the bacterial surface as a result. When binding to biomaterial surfaces,

proteins can change the surface characteristics of the substratum—for instance, the hydrophobicity that is thought to be an important factor in bacterial adherence—and thus either promote or inhibit bacterial attachment (Hogt et al. 1985, An and Friedman 1998, MacKintosh et al. 2006).

Albumin is an essential plasma protein, the antiadherent nature of which has been known for decades (Packham et al. 1969), and the literature provides several studies showing the inhibitory effect of albumin coating on bacterial adherence to bioimplant surfaces in vitro (Zdanowski et al. 1993, Keogh and Eaton 1994, An et al. 1996), and its effect in reducing postoperative infections in vivo (An et al. 1997). Furthermore, some evidence indicates that albumin coating of vascular prostheses, dialysis membranes, and artificial heart valves could have beneficial effects due to such a coating's being antiadhesive and antithrombogenic (Remuzzi and Boccardo 1993, al-Khaffaf and Charlesworth 1996, Hyde et al. 1999). Coating of tympanostomy tubes with HSA has proven effective in preventing early postoperative tube occlusions and undesirable adhesion of proteins and other material to the tubes (Kinnari et al. 2001, 2003, 2004, 2005), although no significant difference between HSA-coated and uncoated tubes emerged in a long-term follow-up of postoperative sequelae (Kinnari et al. 2007). Coating a medical implant with HSA seems to be a safe method. One follow-up study of 200 patients with albumin-coated vascular grafts (al-Khaffaf and Charlesworth 1996) uncovered no disadvantages. Commercially available HSA is manufactured from donor blood, and during this process it is heated at 60°C for hours, which causes inactivation of hepatitis viruses. In general, the safety of HSA use in medical care has been very high (Tullis 1977, Erstad 1996).

In its native state, albumin carries a strong net negative charge that makes it move rapidly in electrophoretic fields, but despite this negative charge, it can bind reversibly to both cations and anions (Tullis 1977). Because of albumin's strong binding affinity, biomaterial surfaces can be easily covered by a durable albumin coat (An et al. 1996, Kinnari et al. 2003). Although the mechanism of albumin's inhibitory effect on bacterial adhesion is unclear, it has been assumed to be based on the changes induced in the hydrophobicity and charge of the substratum surface (Hogt et al. 1985, An and Friedman 1998). As established by scanning electron microscopy (Kinnari et al. 2003), after albumin coating, the roughness of the surface has also been found to decrease, which presumably makes the biomaterial surface less favorable for bacterial adhesion.

2.3.7 Silicone and titanium as otologic implant materials

In ear surgery, silicone and titanium have long served as implant materials. The most common application is the tympanostomy tube that generally consists of silicone or titanium (Bluestone and Klein 1995). Silicone sheets have been useful to line the walls of the tympanum in the surgery for CSOM to prevent development of adhesive otitis media postoperatively (Brackmann et al. 2001), and silicone bands are sometimes used to stabilize middle ear prostheses (Vincent et al. 2005). Titanium has clinically proven to be an excellent auditory ossicular replacement material with good biocompatibility, stability, and low complication rates (Brackmann et al. 2001, Dalchow et al. 2001, Yung 2003, Fisch et al. 2004), and it has also been successful in reconstruction of postauricular mastoidectomy defects (Jung and Park 2004).

2.4 POLYLACTIC- AND POLYGLYCOLIC ACID-BASED COPOLYMERS

2.4.1 Polylactic-, polyglycolic-, and polylactic-glycolic acid

The biodegradable polymers polylactic acid and polyglycolic acid are derived from the cyclic dimers (lactide and glycolide) by polymerization. These polymers are degraded by hydrolysis and enzymatic activity in vivo to monomers (lactic- and glycolic acid) and finally to the end products carbon dioxide and water. Pure PLA degrades and loses its strength very slowly due to its crystallinity and hydrophobicity. Lactic acid exists in two stereoisomeric forms, L- and D-lactic acid, and the stereocopolymers of PLA (derivatives of L-, D-, or DL-lactides) degrade more rapidly than does pure PLA, due to their lower crystallinity (Waris et al. 2004). Pure PGA is a hard, crystalline polymer insoluble in most common polymer solvents that has a high initial strength which nevertheless diminishes rapidly in vivo within a few weeks, due to its susceptibility to hydrolysis (Törmälä et al. 1998). In addition, rapid hydrolysis of PGA releases large amounts of glycolic acid, which can lead to decreased biocompatibility (Böstman and Pihlajamäki 2000, Waris et al. 2004).

Polylactic-glycolic acid is a copolymer synthesized from the corresponding homopolymers (PLA and PGA). Combining PLA and PGA at different ratios allows degradation speed and

other biomechanical characteristics of the PLGA to be regulated. The more PGA that PLGA contains, the faster it is degraded and the greater is its initial strength (Park 1995). PLGA copolymers have relatively low crystallinity, and their physical properties are halfway between those of pure PLA and of PGA. For example, a PLGA 80/20 (80% PLA, 20% PGA) copolymer is substantially amorphous and maintains its mechanical strength for 6 to 8 weeks in vivo (Waris et al. 2004). Subsequently, complete absorption occurs in 1 to 2 years (Eppley and Reilly 1997, Tiainen et al. 2004, Landes et al. 2006a). Several commercially manufactured PLGA products have been precisely engineered for specific uses, simultaneously utilizing the possibility to influence with the copolymer ratio the degradation time and mechanical properties. In recent decades, PLA- and PGA-copolymers have been under intensive bioimplant- and tissue engineering research due to their innumerable potential applications and modifications. Polymer matrices can be reinforced with molecules or bioabsorbable fibers to enhance their mechanical strength, moldability, and elasticity (Törmälä et al. 1998, Lewandrowski et al. 2000). Furthermore, they can serve as porous scaffolds or as carriers of cells, extracellular matrix components, or bioactive agents (section 2.4.4).

2.4.2 Biocompatibility

The biocompatibility of an implanted material is a dynamic process that involves the effect of the host on the material and of the material on the host. Implantation of any synthetic material induces a wound-healing mechanism which is characterized by an inflammatory reaction (Merchant 1989). This non-specific inflammatory response may involve a foreign body reaction or fibrosis (Törmälä et al. 2003). Some characteristics of the implant material may also promote bacterial adhesion to its surface, which in turn may predispose to postoperative implant infection and lead to poor tissue integration and compatibility (Gristina 1987).

The PLA- and PGA-derived implants have a history of more than 30 years of clinical use and have been proven safe and biocompatible materials in the majority of clinical and experimental studies (Böstman et al. 1995, Kallela et al. 1999, Suuronen et al. 2004, Waris et al. 2004, Landes et al. 2006b). Clinically significant complications range from less than 1% up to 10% of the patients, the average, in the large study groups, being around 5%. The peri-implant tissue response seems to continue as long as the degradation continues. It involves slightly elevated leukocyte activity near or on the surface of the degrading material, plus

fibroblast activity with production of collagen and other connective tissue proteins in the outer zone of the interface area (Santavirta et al. 1990, Kontio et al. 1998 and 2005, Pihlajamäki et al. 2006), the latter phenomenon indicating fibrous capsule formation around the implant. These histological findings are similar to those seen during wound healing. In a large retrospective study of 2528 orthopedic patients (Böstman and Pihlajamäki 2000), adverse reactions around the implant included a sterile inflammatory reaction with foreign-body giant cells. In 4.3% of these patients the response was clinically significant, including erythema and discharge, sinus formation, and osteolytic changes at the implant site. The reactions ranged from mild to severe, and four patients developed severe osteoarthritis. Complications were established essentially more with PGA implants (5.3%, n=107) than with PLA implants (0.2%, n=1).

In dog ureters, PLA induces only minimal wall edema, epithelial hyperplasia and destruction, and an inflammatory cell reaction in situ. These reactions subside after the degradation of the stent (Lumiaho et al. 2000). Biocompatibility of a barium sulfate-blended (X-ray-positive) PLA stent in rabbit urethras was good (Isotalo et al. 1999). Multanen et al. (2002) also reported the good biocompatibility of a urethral PLA stent in rabbits. With experimental endotracheal PLA- and PLGA stents, the findings in pigs and rabbits have included some mucosal hyperplasia, epithelial ulceration, and inflammatory reactions around the implant, but good overall biocompatibility of the materials in the trachea. Scanning electron microscopy studies have revealed re-epithelization with ciliated cells of the tracheal wall over the implant (Korpela et al. 1998 and 1999, Robey et al. 2000a, Nalwa et al. 2001). External tracheal PLGA stents in a rabbit model (Robey et al. 2000b) have induced granulomatous inflammation and fibrosis outside the tracheal lumen; in some of these animals endotracheally, subepithelial edema was evident as well as foci of acute inflammation. Re-epithelization of the interior surface was complete in all animals. PLGA has also been used successfully in rabbit laryngotracheal reconstruction (Klein et al. 2005) and vocal cord medialization laryngoplasty (Dufresne and Lafreniere 2000).

PLA-composed vascular stents have proven highly biocompatible in experimental animal studies. Histological findings regarding this implant have been quite similar to those mentioned, including infiltration of chronic inflammatory cells, a mild foreign body reaction, and fibrosis (Hietala et al. 2000, Vogt et al. 2004, Uurto et al. 2007). These stents have also been tested as drug carriers. First, the implant is coated by the drug, or the drug is

incorporated into the implant material by processing (Blindt et al. 1999). Then the drug is delivered locally during the implant degradation. Drug-release kinetics can be regulated by implant pore size. PLA vascular stents containing indometacin have induced less fibrosis (Uurto et al. 2007), and those eluting dexamethasone or paclitaxel have induced less neointimal hyperplasia than have the ones without the drug (Vogt et al. 2004, Uurto et al. 2005). Overall biocompatibility of the stents has been good. Tissue engineering of experimental vascular grafts has involved culturing of smooth muscle cells on a PGA mesh in a bioreactor system (Ratcliffe 2000). After 8 weeks, the mesh was replaced by a smooth muscle cell medial layer. Later, epithelial cells were added to form a two-layered arterial graft, the applicability of which was tested in pigs; the grafts remained functioning for up to 4 weeks.

Feenstra et al. (1984) investigated the suitability of PGA and PLA in myringoplasty in rats and dogs. PGA grafts proved not to be applicable for this purpose because of rapid disintegration of the implant into sharp needles. PLA gave satisfactory results with the rats, but in dogs the grafts succeeded less well, inducing a more marked inflammatory reaction both in the middle ear and subcutaneously. Biocompatibility of PLA in the chinchilla middle ear has been studied by Goycoolea et al. (1991, 1992, 1994), who also developed a new, self-expandable PLA device for antibiotic delivery. Release of ampicillin during the implant degradation remained at therapeutic levels in vitro during a 3-month follow-up, and in vivo efficacy of this implant was evident in otitis-induced cats and chinchillas. Furthermore, the investigators found no inflammatory reaction from the device itself and no evidence of ototoxicity to the organ of Corti. They also documented biodegradation of the device in the chinchilla middle ear in a 3-week follow-up period.

Resorption rate and biocompatibility characteristics of PLA- and PLGA tympanostomy tubes in the guinea pig were determined by Massey et al. (2004). They found that PLA tubes remained longer in the TM than did PLGA tubes, and the biocompatibility of the biodegradable tubes corresponded to that of the control minigrommet tubes. Mild inflammatory changes in the TM occurred in all groups (including the controls), and after resorption of the biodegradable tubes, the TMs healed normally. The end stage of the TMs after healing was found to be histologically similar to that of the non-operated controls. No excessive tympanosclerosis or atrophy of the TMs was observable.

2.4.3 Bacterial adherence

Quite a few studies examine bacterial adherence to pure PLA, PGA, or PLGA surfaces. Polymer surfaces in general possess more hydrophobic than hydrophilic properties (An and Friedman 1998), and this could be assumed to enhance the adherence of many bacterial species to these surfaces. However, contradictory data exist on this topic, as well as data on some other bacterial adherence principles, as mentioned (section 2.3).

Petas et al. (1998) studied the adherence of uropathogenic bacteria (*Proteus mirabilis, Pseudomonas aeruginosa, Enterococcus faecalis*, and *Eschericia coli*) to self-reinforced PGA- and PLA urological spiral stents in vitro. Gold, polyurethane, and latex served as controls. The results showed a more significant correlation between adhesion and bacterial type than with material tested. The authors concluded that the bacterial properties are equally or more important in the adhesion process than are the characteristics of the material. Verheyen et al. (1993) investigated the adherence of *Staphylococcus aureus* and *Staphylococcus epidermidis* to PLA, composite (hydroxyapatite/PLA), and stainless steel. *S. aureus* adhered more to metal and composite than to pure PLA, whereas *S. epidermidis* showed no preference for any of the materials tested. Chen et al. (1997), exposing collagen-, polytetrafluoroethylene-, and PLA membranes to oral bacterial flora, found no differences in bacterial adherence or antimicrobial properties between these materials. Adherence of *S. aureus*, *S. epidermidis*, *E. coli*, and *L. acidophilus* to polymeric biomaterials, among which was PLGA, was explored by Karakeçili and Gümüşderelioğlu (2002), who concluded that the adhesion behavior of *S. aureus* and *S. epidermidis* was independent of the polymeric surface hydrophobicity, whereas less adherence of *E. coli* and more that of *L. lactophilus* occurred on the surfaces with the most hydrophilic properties. Bacterial adherence in this study was tested under static conditions and in a laminar flow cell. Ludwick et al. (2006) examined the adherence of *S. aureus* and *P. aeruginosa* to experimental PLA tympanostomy tubes in vitro. After similar bacterial incubation and conditioning of the tubes, bacterial cultures were taken from PLA tubes and standard fluoroplastic tubes. With both bacteria, the mean bacterial colony count was significantly lower for the PLA- than for the fluoroplastic tube group. The authors concluded that the pure PLA is bacteriostatic. However, no conclusions could be drawn as to mechanism of this proposed characteristic of PLA.

In addition to the studies on bacterial adherence to pure PGA, PLA, and PLGA, a number of studies consider the adherence in vitro of various bacterial species to PLA-, PGA-, and PLGA materials which were antibiotic-blended, -releasing, or which possessed antimicrobial properties (silver nitrate-coated) (Cormio et al. 1997, Multanen et al. 2000a and 2000b, Niemelä et al. 2006). The results in general have shown a clear decrease in bacterial adherence to the pretreated materials in comparison to adherence to non-treated ones.

2.4.4 Applications

Polylactic- and polyglycolic acid-based bioimplants have been successful for decades in CMF-, orthognathic-, and orthopedic surgery, for example as osteosynthetic plates and screws (Suuronen et al. 2000 and 2004, Böstman and Pihlajamäki 2000, Rokkanen et al. 2000, Al-Sukhun et al. 2006, Landes et al. 2006), and as suture materials in all surgeries (Törmälä et al. 1998). Furthermore, antibiotic-releasing screws have been developed to prevent or treat bone infections (Waris et al. 2004). In plastic surgery, PLGA plates have served for reconstruction of the auricle instead of a costal cartilage graft in patients with microtia (Lim et al. 2006). Urethral stents made of PLA, PGA, or PLGA have been in wide clinical use (Tammela and Talja 2003). PLA stents have also been used clinically to treat coronary artery occlusive disease with promising results (Tamai et al. 2000). In addition, successful reduction of neointimal hyperplasia and restenosis of the artery with biodegradable, drug-eluting stents has been documented in experimental studies (Yamawaki et al. 1998, Vogt et al. 2004, Uurto et al. 2005).

Experimentally, PLA implants have protected the bone defects against invasion by surrounding tissues, while the defects have gradually filled with new bone tissue. Based on these studies, whether the pure PGA or PLA has an osteostimulatory effect on bone regeneration has been controversial (Giardino et al. 1999 and 2006, Gogolewski et al. 2000, Nordström et al. 2001, Schmidmaier et al. 2006). Bone tissue engineering and osteogenesis induction in vitro and in vivo have been successful with the use of composites as scaffolds consisting of PLA/PGA and bioceramics (bioactive glass, tricalcium phosphates, and hydroxyapatites) (Blaker et al. 2003, Waris et al. 2004, Hasegawa et al. 2007). Culture of chondrocytes on PLGA in vivo has resulted in neocartilage formation of the exact dimensions of the original scaffold (Baek and Ko 2006); fibroblast culture on PGA scaffold in vitro has also been successful (Kwon et al. 2001). Biodegradable scaffolds as well as growth factor-

releasing degradable biomaterials are likely to come into routine clinical use (Rice et al. 2005, Wildeman et al. 2005). Nanoparticles as potential carriers can be designed for site-specific delivery of many kinds of drugs and macromolecules. During recent years, extensive investigations have explored the possibilities to use biodegradable polymers, especially PLA, PGA, and PLGA, for preparation of nanoparticles (Bala et al. 2004). The targeting capability of nanoparticles is, however, influenced by numerous factors in vivo requiring continuous research on clinical applications in this field.

2.5 RADIOLOGICAL EXAMINATION OF THE MIDDLE AND INNER EAR

2.5.1 Projection radiography

Conventional projection radiography of the ear includes lateral, axial, and semiaxial projections. The pneumatization stage of the mastoid cells and signs of sclerosis or bone destruction can be evaluated to some extent (Cummings et al. 1998). Projection radiography has nowadays been replaced by CT, which is much more accurate and provides exact information on bony structures and cavities in the middle and inner ear area.

2.5.2 Computed tomography

CT is the initial method of choice for imaging the middle ear. The middle and inner ear contain many tiny and thin bony structures adjacent to air-filled spaces, for imaging of which CT is superior to other techniques (Williams and Ayache 2004). Clear visualization of erosion and destruction of bone tissue in pathological situations such as cholesteatoma or COM is essential for diagnostics and treatment planning.

In acute otitis media and mastoiditis, CT shows the fluid- and debris-filled middle ear cavity and mastoid cells with their bony borders (Migirov 2003). Furthermore, CT is the main modality of choice for investigating various manifestations of COM and cholesteatoma; CT explores the extent of bone destruction, its relationships to the surroundings, the state of the auditory ossicular chain, and retractions of the TM (Maroldi et al. 2001). Temporal bone fractures are also revealed by CT (Casselman 1996). Because of excellent visualization of the

ossicular chain, CT should be chosen as the primary imaging method in diagnostics of conductive hearing loss. Such situations include complications of acute otitis media and COM, postoperative ear, trauma, and congenital bony or vascular anomalies such as persistent stapedial artery (Kösling and Bootz 2001, Maroldi et al. 2001, Rangheard et al. 2001, Migirov 2003, Jain et al. 2004, Williams and Ayache 2004). In the imaging of inner ear pathology, the pars petrosus and certain anomalies of the temporal bone, and in differential diagnostics of cholesteatoma or tumors in the temporal bone area, CT may be complementary to MRI and vice versa (Jackler and Parker 1992, Casselman 1996, Czerny et al. 2001, Klingebiel et al. 2002, Curtin 2003).

CT should be performed in both axial and coronal planes either separately or by multislice helical (spiral) CT, in which the X-ray tube continuously rotates around the patient who is simultaneously being moved longitudinally. With multislice helical CT, computer data allow multiplanar reconstruction of images in each preferred plane (Caldemeyer et al. 1999). Slice thickness in the image set can be a minimum 0.5 mm, and imaging should be performed with a high-resolution bone algorithm. For imaging the ear, contrast agents are usually not necessary unless vascularised lesions (such as tumors) and anomalies, or complications of otitis media are suspected (Maroldi et al. 2001). The disadvantage of CT is the patient's exposure to a relatively high radiation dose per examination. Furthermore, it is sometimes necessary to image the ear several times, e.g., pre- and postoperatively or during follow-up. The radiation dose acquired from CT increases cumulatively when repeated. Some controversy exists as to need for routine preoperative CT scanning of cholesteatoma patients (Watts et al. 2000, Yates et al. 2002, El-Bitar et al. 2003). However, with clinical signs of a complicated situation, or in the case of congenital cholesteatoma or revision surgery, preoperative CT examination may be advisable.

2.5.3 Magnetic resonance imaging

MRI is superior to CT in showing liquid-filled areas such as inner ear content and in resolution of soft tissues (Williams and Ayache 2004). If imaging in diagnostics of primary sensorineural hearing loss is necessary, MRI is the method of choice. Furthermore, suspected intracranial or other life-threatening complications of acute otitis media, CSOM, cholesteatoma, or petrositis requires use of MRI, often together with CT (Jackler and Parker

1992, Maroldi et al. 2001). MR angiography replaces the need for digital subtraction angiography (DSA) in evaluation of possible sinus and jugular vein involvement.

MRI is useful in differential diagnostics of petrous apex lesions, cholesteatoma and its recurrences, granulation tissue, cholesterol granuloma, and soft tissue pathology (inflammation, tumors) (Jackler and Parker 1992, Casselman 1996, Kösling and Bootz 2001, Williams and Ayache 2004, Dubrulle et al. 2006). New sequences in MRI seem useful in detecting residual or recurrent cholesteatoma in postoperative follow-up (De Foer et al. 2007, Ketelslagers et al. 2007). In addition, MRI is recommended when exact dimensions of complex conditions affecting the middle ear must undergo assessment, such as extensive cholesteatoma and certain postoperative situations, in relation to the dura mater and intracranial structures (Kösling and Bootz 2001, Maroldi et al. 2001). Any interruption of the tegmen tympani has to be evaluated with MRI for the exclusion of meningocele or meningoencephalocele. MRI should also be the procedure of choice when a middle- or inner ear tumor (like vestibular schwannoma) or other pathology of nerve tissue or labyrinthine content is suspected (Czerny et al. 2001). For diagnostics of glomus tympanicum or an aberrant internal carotid artery, MR angiography is advisable, and jugular bulb anomalies may require MR venography (Maroldi et al. 2001).

An MRI study requires use of a head coil. Images are taken in axial and coronal—in some cases also sagittal—planes to the hard palate, with both T1 and T2 sequences performed. Gd (Gadolinium)-DTPA contrast agent is given intravenously to verify eventual circulation in the object or to enhance contrast between the tissues when necessary (Jackler and Parker 1992, Maroldi et al. 2001, Williams and Ayache 2004). Avoidance of radiation exposure is the great advantage of MRI over CT. However, MRI has patient-dependent limitations: pacemakers and most of the ferromagnetic foreign bodies are not allowed; claustrophobia, lack of patient cooperation, and allergies to contrast agents may also limit MRI use.

2.5.4 Digital subtraction angiography

DSA plays an important role in preoperative planning when treating paragangliomas extending into the middle ear. DSA allows evaluation of stage and extent of tumor vascularisation. Furthermore, DSA and related interventional techniques play an essential role in successful preoperative embolization of these tumors (Maroldi et al. 2001).

2.6 CONE-BEAM COMPUTED TOMOGRAPHY

2.6.1 Technical basis

The CBCT technique was originally developed in the 1990´s for radiotherapy and vascular imaging applications (Saint-Félix et al. 1994, Cho et al. 1995) and was also employed in microtomography of small specimens used in biomedical and industrial applications (Machin and Webb 1994). In the late 1990´s, the technique was first applied to dental, and later to maxillofacial imaging (Mozzo et al. 1998, Arai et al. 1999, Hashimoto et al. 2003, Sukovic 2003, Hintze et al. 2007). With continuous research and technical advancement of the equipment, new applications of CBCT are emerging.

CBCT is based on volumetric tomography data acquired from a two-dimensional detector combined with a 3D X-ray beam. In the CBCT technique, a 360° rotating scan with the X-ray tube and the detector move around the patient's head, which is stabilized in a head-support. Rotation time is between 10 and 40 s, being typically 17 s or more (Robinson et al. 2005, Boeddinghaus and Whyte 2007). Based on the data acquired, the computer software creates a 3D volumetric data set that can be used to reconstruct high-resolution images in axial, sagittal, coronal, or modified planes (Terekado et al. 2000, Araki et al. 2004, Scarfe et al. 2006). In most of the commercially available machines, the patient is in a standing or sitting position during scanning (Fig. 1), although some equipment allows the patient to be in a supine position.

The field of view (FOV) of the machine depends on the model of the scanner and varies from 3 to 20 cm in height and axial diameter (Araki et al. 2004, Robinson et al. 2005). The X-ray tube voltage and current can be adjusted, with different FOV modes for a specified purpose (e.g., facial, panoramic, and implant modes) (Araki et al. 2004). CBCT is particularly well suited for high contrast resolution such as imaging of bone. Due to the lower radiation dose of CBCT compared to conventional CT, its image noise is greater and low contrast resolution poorer (Robinson et al. 2005). Furthermore, X-ray scatter in CBCT limits image quality significantly by reducing contrast and by creating image artifacts (Siewerdsen et al. 2006). CBCT is therefore not yet suitable for routine diagnostic soft-tissue assessment. However, the latest advancements have brought new, better techniques and software algorithms for X-ray

scatter estimation and correction, as well as for improving contrast-to-noise-ratio (CNR) and contrast (Gomi et al. 2006, Siewerdsen et al. 2006, Tu et al. 2006, Graham et al. 2007). In addition, new techniques allow focusing the imaging—and thus the irradiation—onto the region of interest (ROI) only (Wiegert et al. 2005, Cho et al. 2007). The ROI may be only a small part of the FOV of the machine such as a small change in the object during interventional radiology. The ROI imaging techniques allow reduced radiation exposure to the patient, lesser scattering to the detector, and a potential increase in spatial resolution of the reconstructed images.

The volumetric data set involves small 3D cuboid units called voxels. Each voxel represents a specific degree of X-ray absorption, and the size of the voxels determines the resolution of the image. In CBCT equipment, the voxel resolutions are isotropic. Isotropic voxels, equivalent in all three dimensions, result in sub-millimeter spatial resolution that is often much higher than in multislice CT equipment (Scarfe et al. 2006, Boeddinghaus and Whyte 2007). Minimum section distance can be as small as 0.08 mm in some models. Studies comparing accuracy of CBCT with conventional CT units have usually shown a clear advantage for CBCT in imaging small pathologic changes in hard tissues or implants (Hashimoto et al. 2003 and 2007, Sukovic 2003, Winter et al. 2005, Suomalainen et al. 2008).

Data published on the radiation dose with CBCT examination indicates that the skin and effective doses are considerably lower than in conventional CT imaging (Mozzo et al. 1998, Linsenmaier et al. 2002, Hashimoto et al. 2003, Mah et al. 2003, Sukovic 2003, Schulze et al. 2004, Winter et al. 2005, Scarfe et al. 2006). The dose is, however, affected by many factors such as the settings and protocols used as well as the FOV of the equipment (Robinson et al. 2005). In addition, with the low-dose techniques applied in conventional CT, the difference between radiation doses (CBCT vs. conventional CT) can be reduced (Cohnen et al. 2002, Suomalainen et al. 2008). Other advantages of CBCT, compared with traditional CT, include a lower level of metal artifacts in images and smaller, lower-priced, mobile equipment (Scarfe et al. 2006).

2.6.2 Current applications

CBCT technology has undergone significant development in the past few years, and its operative field is continuously expanding. Microtomography with the cone beam technique has been used experimentally for investigation of the bone architecture and mineralization, vasculature, heart valves, tumors, and for adipose tissue quantification (Machin and Webb 1994, Robinson et al. 2005). It has also been useful in experimental endodontology. In clinical use, CBCT has already established its position in dental and maxillofacial imaging as an alternative to panoramic radiography and conventional CT (Sukovic 2003, Scarfe et al. 2006, Boeddinghaus and Whyte 2007). CBCT has proven very accurate in showing details of hard tissues in the maxillofacial skeleton and dental area. It has also been a useful tool for the planning of dental surgery and for evaluation of implant position and postoperative status (Terekado et al. 2000, Ito et al. 2001, Ziegler et al. 2002, Winter et al. 2005, Guerrero et al. 2006, Nickenig and Eitner 2007, Suomalainen et al. 2008). Some evidence suggests that CBCT may be useful in evaluation of the cervical vertebrae, arteriosclerosis of the carotids, and the laryngeal skeleton (Heiland et al. 2007).

The CBCT technique has been applicable to planning (with image guidance) and dose calculation of radiotherapies (Guckenberger et al. 2006, Morin et al. 2006 and 2007). With special algorithms, soft-tissue resolution has been sufficient for imaging the tumors and inner organs to the required extent. Results with CBCT-guided intensity-modulated radiation therapy have been convincing (Chen et al. 2006, Ding et al. 2007). Dietrich et al. (2006) investigated Linac-integrated four-dimensional cone-beam CT for on-line imaging of patients receiving radiotherapy. Their modified system was developed for registering of the breathing phase during image acquisition and for correction of artifacts caused by breathing movements. Based on the data acquired, a respiratory phase-correlated four-dimensional CBCT reconstruction was possible.

Experimental and clinical studies on CBCT for intraoperative image-guidance and digital angiography have been successful. CBCT angiography has been efficient in abdominal interventional procedures (Hirota et al. 2006) and in chemotherapy dose-calculation for head and neck tumors (Kakeda et al. 2007a). Furthermore, it has been useful combined with DSA for imaging and transcatheter embolization in diagnosis and treatment of hepatocellular

carcinoma (Kakeda et al. 2007b). Yang et al. (2007) showed CBCT images of mastectomy specimens to have good tissue contrast, and CBCT of the breast has been anticipated as future technology (Van Ongeval 2007). Experimentally, CBCT has been adequate for intraoperative guidance of head and neck surgery, based on soft-tissue and bony anatomy visualization at radiation-dose levels low enough to allow repeated intraoperative imaging (Daly et al. 2006). Furthermore, intraoperative CBCT has proven useful and accurate in tibial plateau fracture reduction (Khoury et al. 2007), navigated implantation of oral implants after microsurgical bone transfer (Heiland et al. 2008), evaluation of sinus floor augmentation (Blake et al. 2007), and surgery on the frontal recess (Rafferty et al. 2005).

Gupta et al. (2004) presented an experimental prototypical volumetric CT scanner with a flat-panel detector suitable only for ex vivo specimens. They found this prototype to be better than multislice CT in revealing fine osseus structures of the temporal bone. Dalchow et al. (2006a,b) examined cadaver temporal bones and patients with conductive hearing loss with the CBCT technique. They could show precise, high-resolution, and almost artifact-free visualization of the alloplastic middle ear implants in the bones. They also demonstrated CBCT to be useful in showing the cochlear implant in normal position. Compared with intraoperative findings, CBCT had excellent prognostic value in patients with conductive hearing loss in predicting disruption or erosion of the auditory ossicular chain. Thus far, the literature provides no reports, however, on CBCT in routine clinical otologic imaging, and only a few studies on otologic CBCT.

Figure 1. Cone-beam CT (3D Accuitomo).

3
AIMS OF THE STUDY

The aims of the thesis were

I to develop a methodology for measuring and quantifying bacterial adherence and its inhibition by albumin on different implant materials in vitro.

II to study the in vitro adherence to PLGA of *Staphylococcus aureus* and *Pseudomonas aeruginosa* and its inhibition by albumin in comparison to two common otologic implant materials: titanium and silicone.

III to test the biocompatibility of two different PLGA materials in the middle ear.

IV to estimate the accuracy of cone-beam CT in imaging of the temporal bone in comparison to multislice helical CT.

V to evaluate the suitability of cone-beam CT for imaging of an operated temporal bone and of middle ear implants.

4
MATERIALS AND METHODS

4.1 BACTERIAL ADHERENCE STUDIES (I, II)

4.1.1 Plates

Bacterial adherence was tested on uncoated and albumin-coated titanium (I, II), silicone (II), and two different PLGA (II) plates. Before all the experiments, the commercially pure titanium plates sized 5 x 5 x 1.2 mm were polished with a silicon carbide polishing paper up to P 1200, after which, under light microscopy, they all had identical surface structure. In the first study (I), 3 HSA-coated and uncoated titanium plates were exposed to each bacterium; altogether titanium plates numbered 12 in this study. In the second work (II), these numbers were a respective 4 and 16. The silicone plates sized 5 x 5 x 0.5 mm were cut from a commercial silicone sheet (Silatos™, Atos Medical AB, Horby, Sweden) used in surgical otorhinolaryngology. Altogether 16 plates of silicone were exposed to each bacterium, 8 of the plates being HSA-coated and 8 uncoated. The PLGA plates were cut from sheets of two different commercial PLGA types to yield group A of 16 plates sized 5 x 5 x 0.75 mm (LactoSorb®, Walter Lorenz Surgical, Jacksonville, FL, USA) and group B of 16 plates sized 5 x 5 x 0.6 mm (Bionx Implants Ltd., Tampere, Finland). The ratio of L-lactate to glycolic acid was 82% vs. 18% in group A and 80% vs. 20% in group B. The plates of both PLGA groups were exposed to bacteria as described above. In total, 12 plates were included in the first study (I) and 64 plates in the second (II).

4.1.2 Coating of the plates with human serum albumin

Albumin coating of the plates was performed with 1% HSA (Human Albumin SPR 40 mg/ml, Finnish Red Cross Blood Transfusion Service, Helsinki, Finland). The plates were incubated at room temperature (RT) in Eppendorf tubes overnight in 1 ml of 1% HSA per plate. The 1% HSA resulted from diluting 250 µl of purified HSA (40 mg/ml) with 750 µl phosphate-

buffered saline (PBS, pH 7.4). After incubation, the unbound albumin was removed from the tubes by washing them three times with PBS. Thereafter, the plates were air-dried and stored.

4.1.3 Bacteria

Culturing of the bacteria, exposure of the plates, and bacterial staining took place in the laboratory of the Division of Clinical Microbiology, University of Helsinki, Finland.
Staphylococcus aureus (ATCC 25923) was cultured in Todd-Hewitt broth at 37°C overnight under continuous orbital shaking. The bacteria were harvested by centrifugation at 4500 g for 10 min. at RT and washed three times with PBS for 5 min. The bacteria were suspended in PBS to give final concentrations of 1 and 5×10^8 colony-forming units (CFU)/ml, based on optical density at 600 nm.
Pseudomonas aeruginosa (ATCC 27853) was cultured at 37°C overnight on chocolate agar plates made in 19 g/l Müller-Hinton II broth and 20 g/l trypticase soy agar (Becton Dickinson, Cockeysville, MD, USA). The bacteria were collected from the plates and suspended in PBS to give final concentrations of 1 and 5×10^8 CFU/ml, as confirmed by plate counts.

4.1.4 Exposure of the plates to bacteria

Prior to exposure, the uncoated plates were washed once with PBS. Three uncoated and three albumin-coated plates of titanium were incubated in each bacterial suspension at RT for 90 min (I). In Study II, four uncoated and four albumin-coated plates of each material were incubated in the same manner in suspensions of both bacteria at concentration of 5×10^8 CFU/ml. Thereafter, the plates were washed three times with sterile PBS and once with purified water for 5 min. each to rinse away free bacteria and buffer. After this procedure, the plates were air-dried at RT and fixed to object glasses.

4.1.5 Quantification of bacterial adherence

After the bacterial contamination, all plates included in the studies were stained for 2 min. with acridine orange and rinsed with H_2O. On each plate, 10 fields measuring 140×110 µm (1300×1030 pixels) were viewed with the fluorescence microscope Zeiss Axioplan 2 (Carl Zeiss Vision GmbH, München-Hallbergmoos, Germany) at $63 \times /1.25$ magnification, and a

standard FITC filter (fluorescein isothiocyanate) was used to analyze the fluorescence in the field. The fields were photographed digitally with Zeiss AxioCam HRc equipment (Carl Zeiss). The photomicrographs were taken of identical sites on each plate. A rectangular path (1×1.5 mm) was formed around the center of the plate, and 10 photographs were taken at 0.5 mm intervals. To avoid the possible unfocused side area, data analysis in each photograph was outlined to a central 44×44 μm (400×400 pixels) area, from which the quantification of the surface area covered with the adhered, fluorescent bacteria was made. The fluorescent area was counted in square pixels with the picture-processing program Image J (National Institute of Health, Bethesda, MD, USA). A total of 120 digital photomicrographs in the first study (I) and 640 photomicrographs in the second study (II) were analyzed and included.

4.1.6 Pilot studies on bacterial adherence

Before the use of these methods with a larger study material, pilot studies were conducted to test the success of culturing the bacteria and measuring the bacterial adherence. First, culturing of the *S. aureus*, the albumin coating, and the contamination of four titanium plates (two uncoated, two albumin-coated) were tested as described in 4.1.2 to 4.1.4. Because after staining, the microscopic distribution of bacterial coverage on a titanium plate was uniform both on uncoated and albumin-coated plates, the methods could be utilized in the actual studies for *S. aureus*.

After clarification of the methods for *S. aureus* came a pilot study for *P. aeruginos*. The bacteria were first cultured overnight in Lur-β broth, after which two uncoated and two albumin-coated titanium plates were contaminated in bacterial suspension, the concentration of which was estimated to be 5×10^8 CFU/ml. After exposure of the plates to bacteria and staining, microscopy showed that the bacteria were distributed considerably unevenly in patches on the plates. That method was abandoned, and a second pilot for *P. aeruginosa* was conducted: culturing of the bacteria on chocolate agar plates, making the suspension, exposure, and staining of the plates as described above. Two uncoated and two albumin-coated titanium plates were included. In microscopy, the bacterial distribution on the plates was now visually clear and uniform both on uncoated and albumin-coated plates. Finally, these methods were successfully exploited in the actual studies for *P. aeruginosa*.

4.2 EXPERIMENTAL ANIMAL STUDY (III)

4.2.1 PLGA middle ear implants

Two kinds of PLGAs were tested in this study for their biocompatibility in the middle ear of the chinchilla. PLGA (A) plates (L82/G18 PLGA, Lactosorb®, W. Lorenz Surgical Inc., Jacksonville, FL, USA) were bent into an L-shape (thickness 0.75 mm, width 2 mm, longer lap length 3-4 mm, shorter lap length 1-2 mm) or straight cut (thickness 0.75 mm, width 2 mm, length 5-7 mm). PLGA (B) plates (L80/G20 PLGA, Bionx Ltd., Tampere, Finland) were only straight cut (thickness 0.6 mm, width 2 mm, length 5-7 mm), because these plates were structurally more fragile, resulting in difficulties in the bending of small implants.

4.2.2 Test animals

Twenty-five male chinchillas, each weighing approximately 550 g, were purchased from an animal farm (Helsinki, Finland). The animals were housed in individual cages in the same room in the experimental animal unit of the Faculty of Veterinary Medicine (University of Helsinki, Finland). Before the actual experimental study, one animal was killed with an overdose of ketamine for anatomical preparation. The EAC, middle-, and inner ear of this animal were examined under a microscope to clarify the anatomy of these structures in the chinchilla. The animal had a straight EAC and a large TM and middle ear bulla. This observation confirmed the proposed suitability of this species for the study, after which, 24 animals were divided into 4 groups: 10 animals for each PLGA group, 2 animals to be sham-operated, and 2 with no operation.

4.2.3 Experimental surgery and follow-up of the chinchillas

Animals were anesthetized with ketamine 40 mg/kg and xylazine 4 mg/kg intra-peritoneally. During the surgery, norepinephrine (1:1000) was used locally for hemostasis. After anesthesia, both ears of each animal were photographed. The EAC and TM were imaged digitally through an otoendoscope before and after surgery. The right ear of each animal (except in the two control cases) was operated on, whereas the left ear served as a control. A transcanal approach was used, and a tympanomeatal flap was elevated under microscopic

control. A PLGA plate (either A or B) was inserted under the annulus such that the plate was partly under the tympanomeatal flap and partly in the tympanum under the mucosa. Eight animals in each study group received this implant. Two animals in each group were implanted such that the whole straight-cut PLGA plate was placed into the tympanum under the mucosa. In the sham-operated group, the tympanomeatal flap was elevated, but no implant material was inserted. Finally, in all animals, the tympanomeatal flap was repositioned.

Three months after surgery, the animals were anesthetized again as described. The TMs and the skin of the EACs were photographed with the aid of an otoendoscope. At this point, four animals were lost due to complications related to anesthesia; one animal in the PLGA (A) group and three in the PLGA (B) group. Six months after surgery, all animals were killed with an overdose of ketamine. The TMs and the skin of the EACs were photographed. Thoracotomy was performed, and a needle was inserted into the left ventricle. The right auricle was opened, and the abdominal aorta was closed. All animals were perfused transcardially with 0.9% NaCl (200-300 ml), followed by 200 ml of 10% formalin solution. Both temporal bones of each animal were removed for further preparation.

4.2.3 Tissue preparation

In all temporal bones removed, a hole was made in their middle ear bullas. The bones were post-fixed overnight in the same fixative at +4°C and decalcified in 0.5 M EDTA solution at pH 7.4 and at +4°C until the bone was adequately soft for sectioning, typically after 7 to 10 days. Each specimen was dissected under a microscope, and a block containing bony EAC, the TM, the tympanum, and the basal turn of cochlea was isolated. Samples were embedded in paraffin wax and cut into 5-µm sections that were stained with hematoxylin-eosin, van Giesson, and Masson´s trichrome for light microscopy.

4.2.4 Analysis of the digital images

Digital images of the EACs and TMs at four time-points (preoperatively, perioperatively, and at 3 and 6 months after surgery) were analyzed. Presence of TM perforations, progress in healing in the EAC, extrusion of biomaterial, and crusting in the EAC were recorded.

4.2.5 Analysis of tissue samples

For histological evaluation, serial sections of five slides per temporal bone and four high-power fields per slide were analyzed. The inflammatory reaction was evaluated and graded as none-mild-moderate-strong (0-3). The inflammatory cell infiltrates and fibrin deposits around the implant, under the skin of the EAC, and in the tympanal mucosa were blindly evaluated. Degradation of the biomaterial and neo-osteogenesis were checked. The basal turn area of the cochlea was also investigated, for the presence of possible hair-cell damage and any inflammatory reaction. Microscopy was performed with an Axioplan 2 microscope (Carl Zeiss, Jena, Germany), used to capture digital images to be analyzed with AxioVision 3.0 software (Carl Zeiss).

4.3 CONE-BEAM CT IMAGING OF TEMPORAL BONE (IV, V)

4.3.1 Temporal bones (IV, V)

In Study IV, 13 non-operated cadaver temporal bones were imaged with CBCT and multislice helical CT for comparison. The bones were from the temporal bone laboratory collection of the Department of Otorhinolaryngology (HUCH). All the bones had intact tympanic membranes.

In Study V, one non-operated and five postmortem operated and implanted temporal bones were imaged with CBCT. The operations performed were: 1) stapedotomy with dislocated McGee piston prosthesis, 2) stapedotomy with McGee piston prosthesis (normal position), 3) atticotomy with PLGA reconstruction, 4) tympanoplasty with titanium PORP and cartilage, and 5) CWD procedure with PLGA and autologous bone reconstruction of the posterior wall of the EAC in addition to tympanoplasty with titanium PORP. The PLGA plates (LactoSorb®, Walter Lorenz Surgical, Jacksonville, FL, USA) had a PLA/PGA ratio of 82/18% and thickness of 0.5 mm.

4.3.2 Imaging techniques and image reconstruction (IV, V)

The 13 temporal bones (IV) were imaged with CBCT (3D Accuitomo; Morita co., Kyoto, Japan) (Fig. 1) at 2mA, 70kVp, and a FOV of 30 mm in height and 40 mm in axial diameter. The exposure time was 17.5 s, corresponding to the 360˚ rotation time of the scanner. The bones were fixed to the adjustable patient chair at the level of the patient's head so that the focus of the cone-shaped X-ray beam was on the middle ear area (Fig. 2). The computer connected to the 3D Accuitomo digitalized and reconstructed the image data to be displayed as high-resolution images. Slice thickness in this image assessment was 0.5 mm. Subsequently, the bones were imaged with multislice helical CT (Aquilion 16; Toshiba, Tokyo, Japan) with a 180 mA, 120 kVp, and 0.75 s rotation time. Scan length was 6 cm, and the reconstruction FOV was 18 cm. A program for otologic imaging with a bone algorithm was used in the processing and reconstruction of the image data. The reconstructed slice thickness was 0.5 mm.

The one non-operated and five operated temporal bones (V) were imaged with this CBCT equipment using four different tube current and voltage settings: 2 mA/70 kVp, 4 mA/70 kVp, 2 mA/80 kVp, and 4mA/80 kVp. The FOV and rotation time of the scanner were as described above. Slice thickness in the reconstructed images was 0.5 mm.

4.3.3 Evaluation of image quality with contrast-to-noise ratio (IV)

To provide a quantitative assessment of image quality, the CNR was evaluated from the middle ear images, and equivalent images were reconstructed from a section of uniform water background. Contrast was measured as the mean pixel intensity difference between circular regions of interest placed upon the external auditory canal air volume and the bone region around the cochlea. Noise was determined as a standard deviation (1 SD) of the pixel intensity within the circular ROI placed on a water background (axial section image of a water-filled cylindrical plastic bottle with a diameter of 7 cm and length of 19 cm). Image analysis was performed with the ImageJ program (v. 1.34s; National Institutes of Health, Bethesda, MD, USA).

4.3.4 Evaluation of the image quality with CNR (V)

Image quality in this study was evaluated with the aid of a special phantom insert used for CNR analysis. The insert consisted mainly of PMMA (polymethylmethacrylate), had a cylindrical geometry, and could be placed inside a commercially available RSVP phantom (The Phantom Laboratory, Salem, NY, USA). The plastic shell of the RSVP phantom corresponded to the surface anatomy of the human head, and the phantom could be filled with water to simulate the physical attenuation characteristics of an in vivo situation. For CNR analysis of this study, the insert was positioned close to the RSVP head's ear and surface so that the holes of the insert containing teflon and air were in the area of the imaginary middle ear and towards the surface of the RSVP. Teflon was used to simulate the bone tissue, and air to simulate the air spaces in the middle ear. CBCT (3D Accuitomo; Morita co., Kyoto, Japan) imaging of the phantom was conducted with the same four imaging protocols described above for the bones (4.3.2) to compare the influence on the CNR of different protocols. The FOV of 30 x 40 mm was centered on the phantom insert. The scanner provided 3D data with isotropic resolution of $0.12 \times 0.12 \times 0.12$ mm^3. For the image quality analysis, axial slices of 1 mm in thickness were exported in DICOM (Digital Imaging and Communications in Medicine) format.

The CNR of two materials was calculated as the difference between the signals measured for each material divided by the image noise according to the equation:

$$\mathrm{CNR} = \frac{\mathrm{Signal}_1 - \mathrm{Signal}_2}{\mathrm{Image\ noise}}$$

The average intensity value measured inside a certain region of interest was considered as signal and the standard deviation of the intensity values inside the region as noise for the material. Image noise was calculated as the arithmetic average over the noise obtained from the two materials considered. CNR was calculated for teflon as well as for air against the PMMA background. For determination of the signals and noises for teflon and air, the ROI was outlined to an area of 40 x 40 pixels. The PMMA background region was limited to a square of 80 x 80 pixels. Analysis was performed for each axial slice of an image set, in which the teflon and air regions could be seen, and the final CNR was assumed to be the

average of the single-slice CNRs. Slices in which partial volume artifacts from the top or bottom plates were visible were excluded from analysis.

4.3.6 Analysis of temporal bone images (IV, V)

In Study IV, 16 clinically and surgically important landmarks in the middle and inner ear were selected for assessment and comparison (Table 2). The conspicuity of the objects in the CBCT and the helical CT images were evaluated according to a modified Likert scale (1=not seen or absent; 2=poorly seen or not diagnostic; 3=clearly seen). In addition to the comparison of scores of individual landmarks, total scores and scores for subgroups forming a specific focus of clinical interest were compared. The subgroups were: the subgroup of joints (incudomalleolar and incudostapedial), stapes structures (head, crura, footplate), and the structures around stapes (tympanic sinus, facial recess, pyramidal eminence). Analysis of all images was performed in the same session by two otologists and one radiologist.

The temporal bone images of Study V were analyzed systematically by the same two otologists and one radiologist. Based on the evaluation, the imaging protocols for the best result in object visualization were graded, and visualization of surgical landmarks and positions of the middle ear implants assessed.

Table 2. Structures evaluated in the CBCT and helical CT images (IV).

Middle ear	Inner ear
Scutum	Modiolus
Sinus tympani	Oval window
Facial recess	Cochlear aqueduct
Pyramidal eminence	Vestibular aqueduct
Cochleariform process	
Incudomalleolar articulation	
Incudostapedial articulation	
Stapes crura	
Stapes capitulum	
Stapes footplate	
Incus long processs	
Petrotympanic fissure	

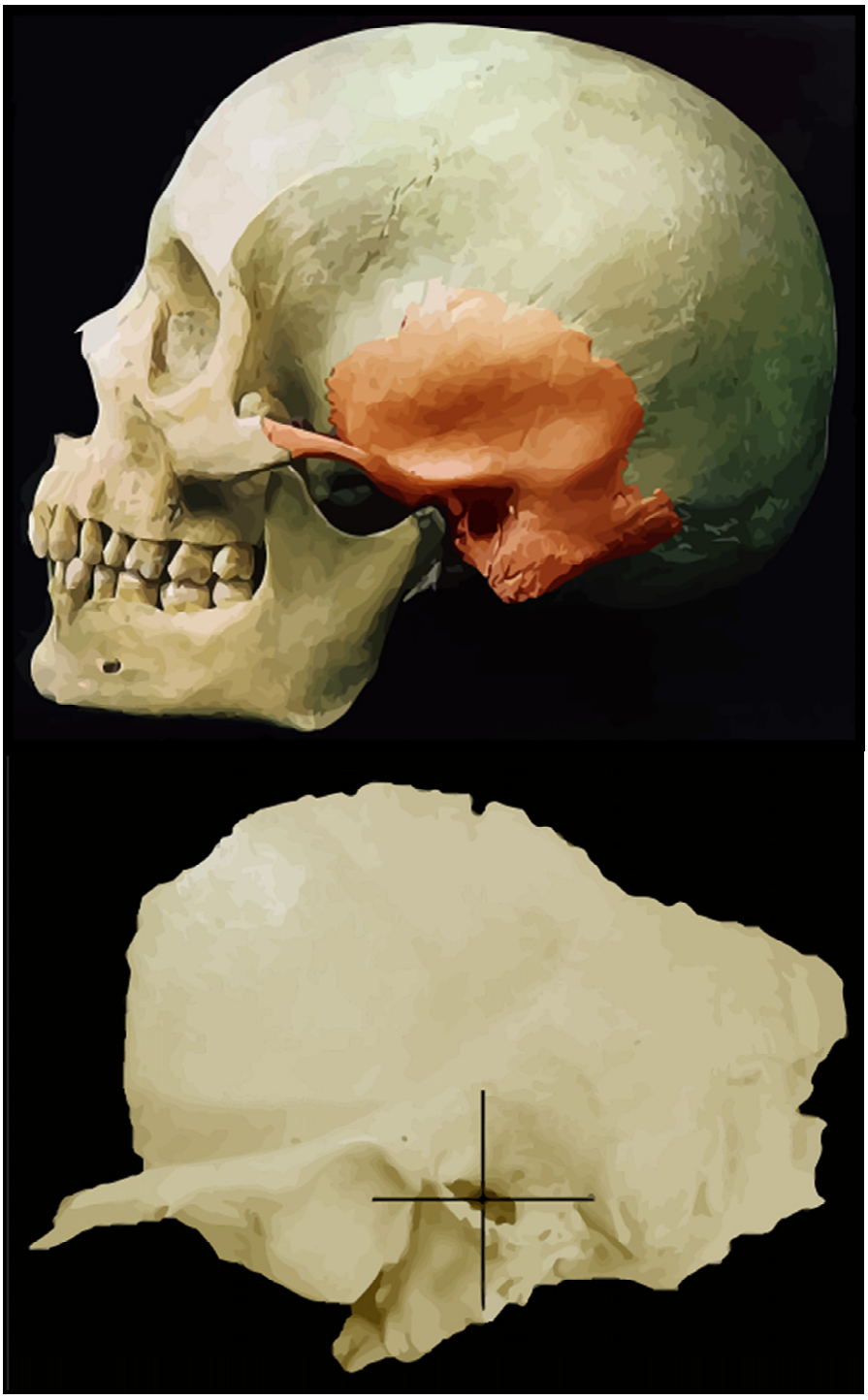

Figure 2. Top; anatomical demarcation of the temporal bone in the skull. Bottom; site of axial and coronal target beams adjusted to the region of interest for imaging of the middle ear of the left temporal bone with CBCT (3D Accuitomo).

4.4 STATISTICAL METHODS

In the first bacterial adherence study (I) and in the CBCT study (IV), Student's t-test was used to compare the results between study groups. In the second study (II), the values of study groups did not conform to the normal distribution, based on the histogram analysis, and the non-parametric Mann-Whitney U-test was selected for the statistical comparison. In the animal study (III), the χ^2 test was used to compare the intensities of tissue reactions caused by the two different PLGAs. The criterion for statistical significance was $p < 0.05$.

4.5 ETHICS

The animal study (III) was approved by the Local Ethics Committee for Animal Experiments, HUCH, University of Helsinki, Finland, and by the Provincial State Office of Southern Finland. Animal experiments were conducted in accordance with the European Convention (1986) guidelines. The use of cadaver temporal bones (IV, V) was approved by the Ethics Committee of the Department of Otorhinolaryngology (HUCH, Helsinki, Finland).

5
RESULTS AND COMMENTS

5.1 BACTERIAL ADHERENCE STUDIES (I, II)

5.1.1 Bacterial adherence to titanium surfaces (I)

The mean coverage of *Staphylococcus aureus* of the uncoated plates was 1.6% (95% confidence interval, CI, 1.1-2.0%) at the 1×10^8 CFU/ml suspension concentration and 6.5% (95% CI 5.3-7.6%) at the 5×10^8 CFU/ml concentration. The corresponding values with the albumin-coated plates for *S. aureus* were 0.22% (95% CI 0.16-0.28%) and 0.25% (95% CI 0.2-0.3%). Adherence was inhibited by 82% at the 1×10^8 CFU/ml concentration ($p < 0.05$) and by 95% at the 5×10^8 CFU/ml concentration ($p < 0.05$).

The mean coverage of *Pseudomonas aeruginosa* of the uncoated plates was 5.0% (95% CI 4.3-5.7%) at the 1×10^8 CFU/ml suspension concentration and 25.4% (95% CI 23.4-27.3%) at the 5×10^8 CFU/ml concentration. The corresponding values with the albumin-coated plates were 3.3% (95% CI 2.5-4.0%) and 16.8% (95% CI 14.8-18.8%). The adherence was inhibited by 29% at the 1 x 10^8 CFU/ml concentration ($p = 0.09$, not significant) and by 37% at the 5×10^8 CFU/ml concentration ($p < 0.05$).

The results showed a significant reduction in the adherence of *S. aureus* and *P. aeruginosa* on albumin-coated titanium compared to uncoated titanium at higher bacterial concentrations.

5.1.2 Bacterial adherence to PLGA, silicone, and titanium (II)

The mean coverage of *Staphylococcus aureus* on uncoated PLGA (A) was 3.35% (95% CI for median 2.35-3.76%), and 0.22% (95% CI for median 0.12-0.24%) on albumin-coated plates. For PLGA (B), the values were respectively 7.62% (95% CI for median 4.67-7.87%) and 1.18% (95% CI for median 0.43-1.22%). For silicone, the corresponding values were 4.90%

(95% CI for median 3.95-5.70%) and 0.61% (95% CI for median 0.53-0.67%), and for titanium 10.58% (95% CI for median 6.77-13.13%) and 0.33% (95% CI for median 0.25-0.39%) (Fig. 3). Albumin coating inhibited the adherence by 93.4% on PLGA (A), 84.5% on PLGA (B), 87.6% on silicone, and 96.9% on titanium (Fig. 4). The decrease in the adherence was significant in all groups ($p < 0.0001$). When compared, most of the adherence differences between the test materials were significant ($p < 0.05$), except for uncoated PLGA (B) vs. silicone ($p = 0.201$) and titanium ($p = 0.117$), and for albumin-coated PLGA (B) vs. silicone ($p = 0.665$) and titanium ($p = 0.050$).

The mean coverage of *Pseudomonas aeruginosa* on uncoated PLGA (A) was found to be 12.73% (95% CI for median 8.85-15.40%), and 6.16% (95% CI for median 4.08-7.62%) on albumin-coated plates. For PLGA (B), the values were respectively 11.19% (95% CI for median 6.41-11.58%) and 8.55% (95% CI for median 3.19-9.62%). For silicone, the corresponding values were 16.94% (95% CI for median 12.12-20.86%) and 4.54% (95% CI for median 1.87-5.72%), and for titanium 40.45% (95% CI for median 36.66-42.88%) and 17.78% (95% CI for median 14.84-21.20%) (Fig. 5). The inhibitory effect of albumin on the adherence was significant for each material, the mean inhibition rate being 51.6% for PLGA (A) ($p < 0.0001$), 23.6% for PLGA (B) ($p < 0.05$), 73.2% for silicone ($p < 0.0001$), and 56.0% for titanium ($p < 0.0001$) (Fig. 4). Again, most of the adherence differences between the materials were significant ($p < 0.05$), except for uncoated PLGA (A) vs. PLGA (B) ($p = 0.062$) and silicone ($p = 0.252$), as well as for albumin-coated PLGA (A) vs. PLGA (B) ($p = 0.513$) and PLGA (B) vs. silicone ($p = 0.366$).

As in Study I, albumin coating of the plates induced a significant decrease in the adherence of *S. aureus* and *P. aeruginosa* to the materials tested. Furthermore, the highest adherence was found on titanium plates with both bacteria, and with albumin coating the differences between the materials diminished. On average, no more bacterial adherence occurred on the PLGA plates than on silicone and titanium.

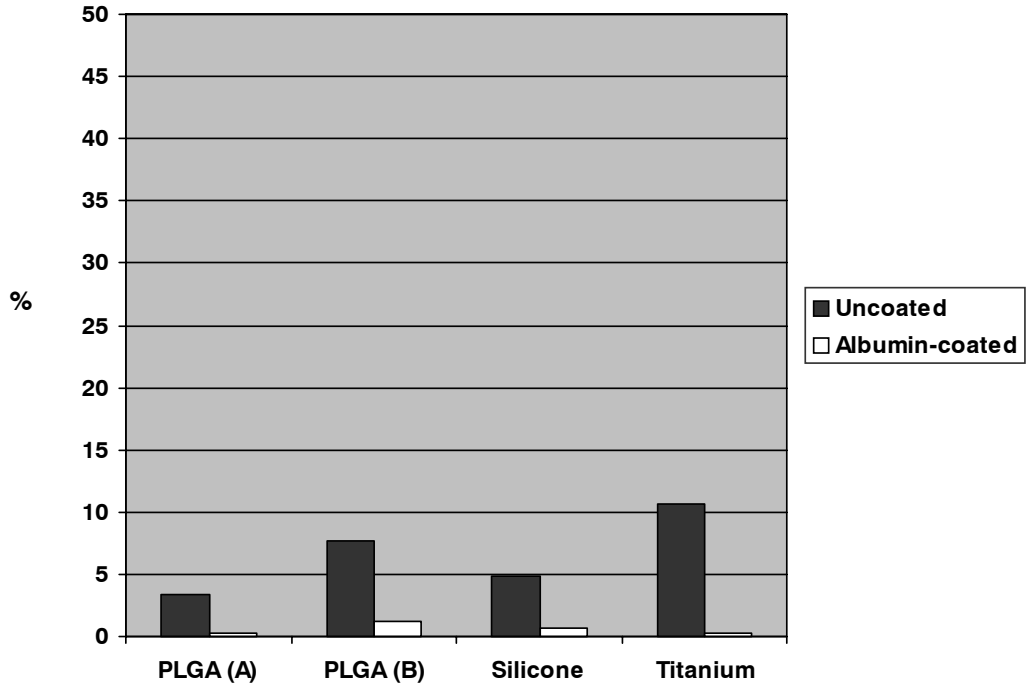

Figure 3. Mean percentage coverage of *Staphylococcus aureus* of the material surfaces (II).

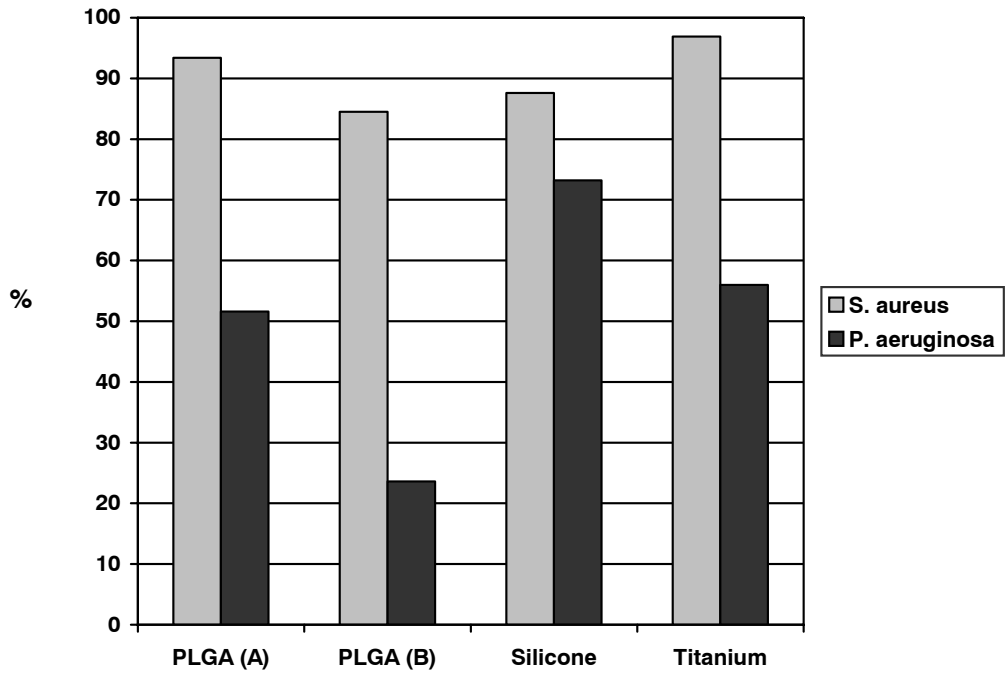

Figure 4. Mean percentage inhibitory effect of albumin on adherence of *Staphylococcus aureus* and *Pseudomonas aeruginosa* to materials tested (II).

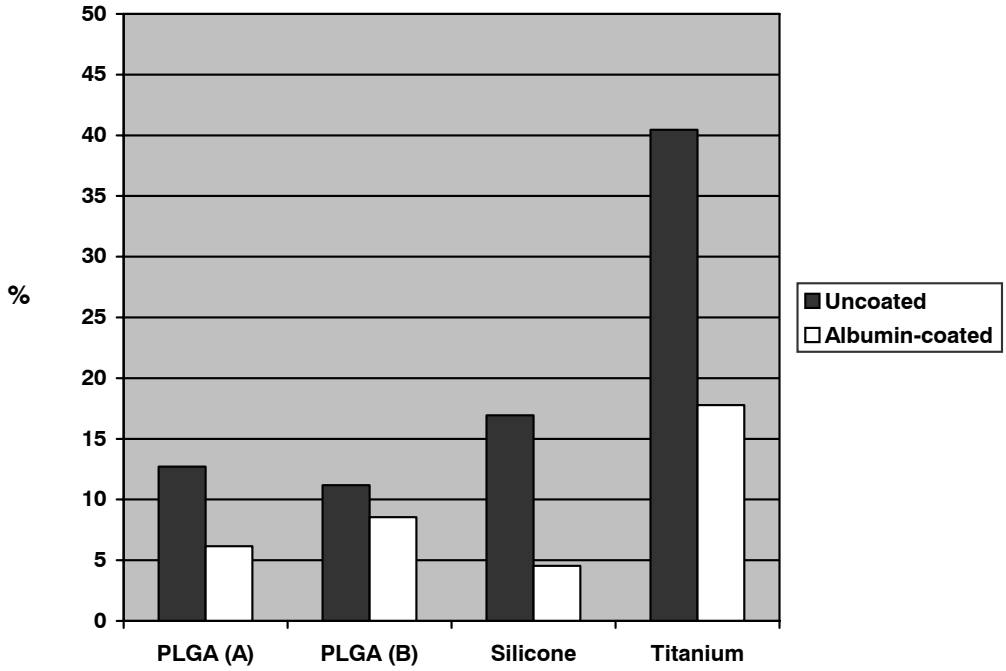

Figure 5. Mean percentage coverage of *Pseudomonas aeruginosa* of material surfaces (II).

5.2 EXPERIMENTAL ANIMAL STUDY (III)

Clinically, all the ears of the animals perioperatively were healthy. In analysis of the otoendoscopic images taken preoperatively, perioperatively, and at 3 and 6 months after surgery, no perforations of the TM, infections of the EAC, or signs of otitis media were observable. At 3 months, images showed some crusting in the EAC, but neither perforations of the TM nor extrusion of the implant material. At 6 months, very minor crusting in the EAC had occurred, but in all operated animals the skin was intact. Neither granulation nor obvious inflammatory changes were present in the EAC, and the TMs were healthy.

In histological samples, both implanted PLGA materials were mostly degraded, with some capsulous fibrin formation present around the PLGA plates. A small amount of inflammatory cell infiltrates surrounded some of the degrading material. These cell infiltrates were evident mainly in the degrading implant itself or on its surface facing the host tissue. They contained polymorphonuclear cells, mainly heterophils, but also some macrophages and lymphocytes.

In the surrounding skin or in the middle ear mucosa, no or at most mild inflammation had appeared. A few of the samples showed coccoidal bacterial colonization of the implant, but the inflammatory reaction in these cases was similar to that observed in the implants free of bacterial colonization. No hair cell damage or inflammatory reaction occurred in the area of the basal turn of the cochlea. Comparison of the degree of the inflammatory reaction between the two PLGA groups disclosed no significant difference ($p = 0.157$). No neo-osteogenesis in the samples was visible.

The results showed no clinical complications of PLGA implantation in the chinchilla middle ear, TM, or EAC. Histologically, at most a mild inflammatory reaction with some fibrous capsule formation was observable around the implants. These findings indicate the good biocompatibility of PLGA implant in the middle ear in an animal model.

5.3 CONE-BEAM CT STUDIES (IV, V)

5.3.1 Comparison of cone-beam CT with multislice helical CT (IV)

When scores of individual structures and subgroups were compared, no significant difference existed between imaging methods ($p > 0.05$), nor any significant difference between total scores for helical CT and CBCT ($p = 0.9340$). The structures evaluated (Table 2) were mostly clearly visible in the CBCT images (Figs. 6 and 7). On average, visualization of the cochlear and vestibular aqueducts was poor with both CBCT and helical CT.

With CBCT, the estimated mean radiation dose of the imaged section was 1.4 mGy, based on the standard dosimetric CT measurement set-up applying cylindrical head phantom geometry with 16 cm axial diameter. According to this physical dose estimation, the calculated effective dose was 13 μSv, which corresponds to the effective dose of half of a PA thorax radiograph. With multislice helical CT, the mean physical dose of the imaged section was 25.8 mGy, recorded from the scanner console. The effective dose was 0.6 mSv, calculated with the CT-EXPO program using the ADAM male anthropomorphic human model (Stamm and Nagel 2002). The CNR was more than 50% lower in CBCT than in multislice helical CT, but still adequate for the diagnostic task.

The results showed that diagnostic imaging of the middle ear is possible with CBCT and at least as accurate as with multislice helical CT. The estimated effective radiation dose of the CBCT was over 40-fold lower than that of helical CT in this setting.

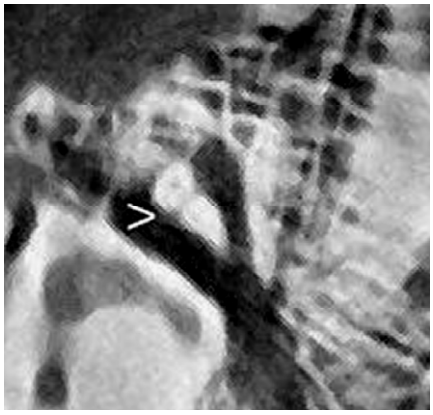

Figure 6. Incudostapedial joint imaged by CBCT (IV). Arrowhead: the joint; axial view.

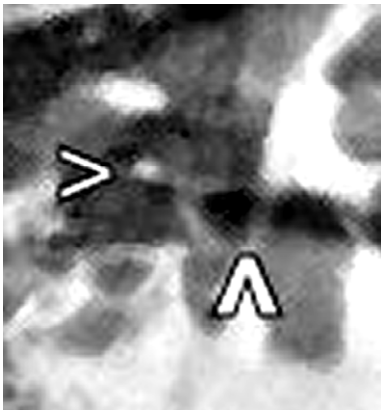

Figure 7. Stapes imaged by CBCT (IV). Thin arrowhead: head, and thick arrowhead: footplate of the stapes; coronal view.

5.3.2 Imaging of the phantom insert and operated temporal bones with CBCT (V)

The best CNRs in the phantom images were achieved with a tube voltage of 80 kVp and a current of 4 mA with both teflon and air. Based on evaluation of the bone images as well, the highest image quality was considered to be with this protocol. With all the temporal bones, image quality was good and of diagnostic value. The middle ear implants and their positions were clearly identified, and the dislocation of the piston prosthesis was clearly visible. In the images of all six temporal bones, the clinically important structures of the middle ear area could be identified. The PLGA plates used in the reconstructions were X-ray negative (Fig. 8).

The results of this study showed that CBCT imaging of operated and implanted temporal bones was successful. With this technique, visualization of the middle ear implants and the auditory ossicular chain is clear, making diagnostic evaluation of these possible.

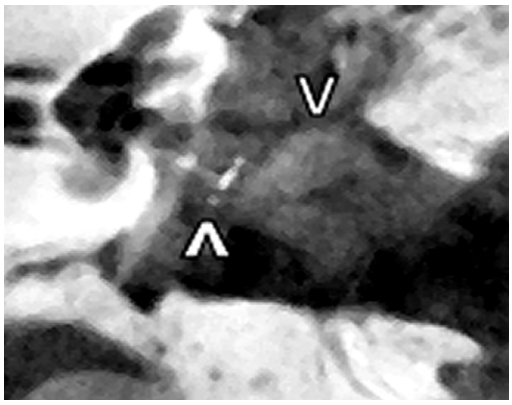

Figure 8. The postoperative situation after tympanoplasty with titanium PORP, CWD procedure, and posterior EAC wall reconstruction imaged by CBCT (V); coronal view. In addition to bone chips and paté, PLGA plates have been used in the reconstruction. Thick arrowhead: PORP; thin arrowhead: site of the canal wall reconstruction.

6
DISCUSSION

The need is constant for improvement of surgical techniques in reconstructive middle ear surgery. Surgical treatment particularly of COM and cholesteatoma pose a challenge to every otologist. In the treatment of adhesive otitis media, results are often poor despite attempts to restore a functional aerated tympanum, and lack of approriate autologous implant material may complicate reconstruction in cholesteatoma surgery. Consequently, synthetic implants are often necessary for providing structural and functional support. An ideal implant material in this context would be biocompatible, unlikely to cause postoperative infections, and suitable for reconstructive purposes in the ear. Furthermore, there should be no need for an implant removal operation. Perioperative decisions of the surgeon play an important role in the successful treatment because of the individual circumstances of every middle ear operation. Therefore, having the option of an implant material with intraoperatively adjustable properties such as pliability and plasticity would be highly desirable.

Polylactic- and polyglycolic acid-based biodegradable copolymers have long been in clinical use in implant surgery and may be suitable for reconstruction of the middle ear and the posterior wall of the EAC. Thus far, they have not been used in human middle ear surgery, however, and reports on their experimental use in the ear are few (Feenstra et al. 1984, Goycoolea et al. 1991,1992,1994, Massey et al. 2004). Studies II and III of this thesis focused on PLGA, and the goal was to discover the biocompatibility and suitability of this material in the middle ear and EAC.

Assessing the severity and extent of COM or cholesteatoma, and planning surgical treatment of these diseases may require CT imaging. Furthermore, CT examination may be necessary in evaluation of a postoperative situation or in follow-up. Although CT is an excellent diagnostic tool, its safety for the patient is not optimal because of relatively high radiation exposure. Because a wide consensus exists among clinicians as to the importance of limiting cumulative radiation dose to a minimum, especially when imaging children, new techniques offering better safety without compromises in diagnostic quality are essential. Studies IV and V were

inspired by the good results with CBCT in imaging of limited areas with reasonable irradiation. Although some have reported otologic imaging with CBCT (Dalchow et al. 2006a,b), more studies should establish the position, indications, and settings for clinical CBCT in this field. A comparative study revealed the diagnostic accuracy of the CBCT in relation to the conventional CT (IV). In addition, applicability of CBCT to imaging of middle ear implants and postoperative ear was clarified (V).

6.1 BACTERIAL ADEHERENCE STUDIES (I, II)

The bacteria chosen for the adherence studies were two typical pathogens involved in CSOM and in a postoperative ear infection: *Staphylococcus aureus* and *Pseudomonas aeruginosa*, whose adhesion to biomaterial surfaces in vitro we studied and compared. Because chronic implant infections lead to medications, hospitalizations, re-operations, increased morbidity and mortality, and tremendous financial costs (Darouiche 2004, Lynch and Robertson 2008), every effort is necessary to prevent such postoperative infections. Antibiotic prophylaxis cannot, however, rule out bacterial adherence and biofilm formation on implant material in vivo (Keane et al. 1994, Morris et al. 1999, Lynch and Robertson 2008). Based on the literature, albumin coating of the biomaterial surface as a potential inhibitor of bacterial adherence, and thus as a preventive procedure of postoperative infection, was also tested in these studies.

The goals of Study I were to develop an appropriate method for quantifying bacterial adherence on titanium plates in vitro and to test the effect of albumin coating of the plates on bacterial adherence to the titanium surface. With the methods used, quantification of adherence to the plates was possible to determine reliably, since fluorescent staining of the bacteria provided a clear view of bacterial coverage in microscopy. The results were uniform for the bacterial species, although the inhibitory effect of albumin was more evident for *S. aureus* than for *P. aeruginosa*. This difference is most apparently related to the adherence characteristics unique to each bacterial species (An and Friedman 1998); e.g., bacteria with fimbriae or flagellae or both (like *P. aeruginosa*) are able to adhere more easily than are ones without fimbriae (Petas et al. 1998, Morris et al. 1999). The results showed the clear inhibitory effect of albumin coating on bacterial adherence of *S. aureus* and *P. aeruginosa* to the titanium surface.

The results of Study II again clearly showed a uniform, significant inhibitory effect of the albumin coating on bacterial adherence. Adherence differences between materials diminished after the albumin coating, consistent with the findings of the universal antiadherent nature of albumin (Packham et al. 1969, Remuzzi and Boccardo 1993, Zdanowski et al. 1993, An et al, 1996, Kinnari et al. 2001). Of the materials tested, titanium allowed the highest adherence for both bacteria, while less adherence occurred on PLGA- and silicone surfaces. The reasons may be related to the roughness and hydrophobicity of the titanium surface. Surface roughness has been considered an essential factor in the bacterial adhesion process (An and Friedman 1998, van de Belt et al. 2001). Under light microscopy, titanium surfaces appeared to be the roughest of all the test materials.

Furthermore, *Staphylococcus aureus* has been shown to have a preference for metal surface in vitro and in vivo, and to be the dominant microorganism associated with infected metal implants (Barth et al. 1989, Verheyen et al. 1993, An and Friedman 1998). Verheyen et al. (1993) also showed *S. aureus* to have a preference for metal (stainless steel) over PLA and composite (PLA/hydroxyapatite). Metal surfaces in general possess a hydrophilic character (An and Friedman 1998), and the majority of *Pseudomonas aeruginosa* strains have been shown to manifest hydrophilic properties (Hostacká et al. 2006). Keeping in mind the proposed general rule that bacteria with hydrophilic properties prefer hydrophilic surfaces (An and Friedman 1998), this observation may explain the results with *P. aeruginosa* in this respect. However, different strains of *P. aeruginosa* have shown essential distinctions in hydrophobicity, exopolysaccharide coat, and the expression of fimbriae and flagellae types (Elsheikh et al. 1985, Spangenberg et al. 1998, Li and Logan 2004). Furthermore, many reports state that the substratum or bacterial surface hydrophobicity has little or no effect on adherence (Sobel and Obedeanu 1984, Elsheikh et al. 1985, Hogt et al. 1985, Verheyen et al. 1993, Karakeçili and Gümüşderelioğlu 2002, Palmer et al. 2007). Because of complexity, unknown factors, and controversies over the bacterial adhesion process, the data acquired in this study can lead to no conclusions as to the reasons for species-dependent bacterial behavior on different materials. One hypothetical reason for titanium's being the most adherent test material in this setting may be the degree of its surface roughness, greater than for other materials.

The focus of interest in Study II was in the PLGA materials and their characteristics in relation to common otologic implant materials. PLGA was chosen because of its being representative of both PLA and PGA, and two different PLGAs were used to exclude potential bias in the results. Two major questions arise regarding PLGA in this context. First, how does the degradation process in vivo affect the surface properties and bacterial adherence of PLGA? Second, do the degradation products generated in a biological environment have any bacteriostatic influence in situ? It has been suggested that degradation of the underlying material to which the bacteria are attached results in the release of bacteria, but numerous adhesive contacts would keep the bacteria on the surface, while individual contact points may be broken and—subsequently—re-form on the next exposed polymer (Stickler 1996, Petas et al. 1998). While the principles of bacterial adherence on the degrading material remain to be discovered, it is, however, justified to state that biodegradable polymers provide only a temporary substrate for bacterial colonization, not one lasting until the end of the degradation process.

Ludwick et al. (2006), who investigated the attachment of *S. aureus* and *P. aeruginosa* to experimental PLA-tympanostomy tubes by incubating the tubes in bacterial suspensions for 48 h, found significantly lower counts of both bacteria on the PLA tubes than on the control fluoroplastic tubes. They concluded that PLA has an apparent bacteriostatic quality that is possibly related to its acidic nature. However, Petas et al. (1998) found no evidence in vitro for this hypothesis, according to which the degradation products of PLA or PGA would create an acidic microenvironment unfavorable for bacterial growth and adhesion during degradation; the follow-up in that study was up to 28 days. They suggested that the acidic potential of the metabolites would be too low to induce a local decrease in pH, or that the change in pH would be small enough—due to the slow degradation rate—to be quickly neutralized by the liquid medium. On the other hand, while some reports support the theory that rapid degradation of pure PGA reduces implant biocompatibility by releasing significant amounts of glycolic acid (Böstman and Pihlajamäki 2000), it is obvious that this issue still remains under debate.

Since the results of Studies I to II were similar with both bacteria, they can be considered reliable. However, because of the complexity and multiple contributory factors of the bacterial adhesion process in vivo, conclusions based on the results of these in vitro studies should be made with caution. First, the in vitro conditions differed markedly from an in vivo

situation with regard to bacterial concentration, temperature, and physicochemical and tissue-specific factors in living tissue. Second, these circumstances also lacked certain competitive factors for bacterial adhesion, such as the presence of other microbes, proteins, and the host's immune mechanisms. However, this model may be considered sufficient and reliable for suggestive results. The literature provides numerous studies and conclusions on biomaterials based on in vitro findings, and, concerning bacterial adhesion, these have been consistent with in vivo findings (Barth et al. 1989, An et al. 1996 and 1997, al-Khaffaf and Charlesworth 1996, Kinnari et al. 2001, 2004, 2005).

6.2 EXPERIMENTAL ANIMAL STUDY (III)

The goal of this study was to determine the suitability of PLGA in experimental ear surgery. Since the chinchilla has been a successful model for experimental ear surgery (Amoils et al. 1992, Downey et al. 2003, Siedentop et al. 2004, Spiegel and Kessler 2005), that animal was chosen also for this study. Anatomical preparation revealed the chinchilla to have a straight EAC and a large TM and middle ear bulla, confirming the suitability of chinchillas for the experiment. PLGA was chosen as the implant material, because, first, it represents both PLA and PGA copolymers. Second, commercial PLGA products have a resorption time (1-2 years) suitable for testing the hypothesis of this study. Pure PGA has a high degradation rate, and its biocompatibility has been reported to be lower than that of PLA (Böstman and Pihlajamäki 2000). Pure PLA in turn degrades very slowly, which presumably would not be a goal for such implant in the ear. In addition, in ear surgery, the implant mechanical strength required is far from that of the osteosynthetic plates used in orthopedic and CMF surgery. Third, PLGA has a capacity to be easily and intraoperatively reshaped by heating, which is important when reconstructing such structures as the posterior wall of the EAC according to the dimensions of each individual's anatomy.

PLGA plates were inserted under the skin of the EAC (in contact with bone) and the mucosa of the tympanic cavity. Neither in clinical follow-up nor in histological samples were any major adverse responses to the implantation evident. The mild inflammation with minor fibrosis was as expected and in accordance with reports on PLGA biocompatibility. Nor did any toxic effects on the inner ear occur. These results confirm the suitability of PLGA in ear surgery in a chinchilla model and support the findings of Goycoolea et al. (1991, 1992, 1994),

who also used the chinchilla in studies of a PLA-based drug-delivery device. Furthermore, Massey et al. (2004) investigated PLA- and PLGA tympanostomy tubes in guinea pigs with good results. Less successful results occurred with PLA grafts in myringoplasty of mongrel dogs, however, (Feenstra et al. 1984), as PLA induced more marked inflammatory reaction than in rats in that study. Results from an animal model should be considered preliminary and not with certainty applicable to human beings. Because knowledge of biocompatibility of PGA, PLA, and PLGA in the middle ear is scarce, more animal research is perhaps needed to verify their suitability in this regard. On the other hand, vast clinical experience in surgery using these materials routinely has demonstrated their good biocompatibility, which favors conducting of prospective studies on use of these polymers in the human ear.

The temporary and non-magnetic nature of a biodegradable PLGA implant reduces the probability of long-term problems compared to those of permanent non-degradable biomaterials. On the other hand, because of the provisional character of biodegradable polymers, they would be suitable for specified purposes only. One potential application would be a biodegradable scaffold in the myringoplasty, where the requirements for functional temporary graft include sufficient mechanical strength, softness and pliability, surviving until complete regeneration of migrating epithelium from the membrane remnants, and a biocompatibility that in particular allows attachment of neo-epithelium to the implant surface. The mild fibrosis produced in the degradation may strengthen the neo-membrane and function as a substitute for the absent collagen middle layer. Alloplastic material instead of autologous cartilage or temporal fascia can reduce operation time; the implant can have a predictable resorption rate and can serve in situations where alloplastic material use is justified, for instance, in congenital or atelectatic ears and subtotal perforations with loss of the malleus (Feenstra et al. 1984). In surgery for COM or cholesteatoma, postoperative medialization of the TM and collapse of the tympanum is a danger. A biodegradable stent supporting the TM at the annulus might prevent the TM's intense retraction after surgery. Again, fibrosis resulting from the degradation may provide additional support, especially in the long term after implant dissolution.

In reconstruction of the posterior wall of the EAC and in mastoid obliteration, numerous techniques have been applicable with both biological and synthetic materials, but no single combination has proven ideal for reliable reconstruction of the posterior canal wall anatomy (Black 1995, Leatherman ad Dornhoffer 2002). Modified PLA- or PLGA plates placed under

the skin and cartilage against the bone chips and paté may be useful in giving structural support and preventing collapse and cavity formation in the wall during healing. The fibrosis induced may strengthen the effect. PLA implants covering bone defects have prevented the invasion of the soft tissues into the neo-osteogenesis area (Giardino et al. 2006, Schmidmaier et al. 2006). What is still controversial is whether pure PLA has an osteoinductive effect. Meanwhile, bioglass possessing excellent biocompatibility has not only served as a scaffold for bone regeneration but also stimulated osteoblast activity and neo-osteogenesis. Furthermore, bioglass also has a bacteriostatic quality (Peltola et al. 1998, Aitasalo et al. 2001, Blaker et al. 2003, Stoor and Grénman 2004, Stoor et al. 2006). Consequently, based on promising results with the use of bioglass in posterior wall reconstruction (Reck and Helms 1985, Leatherman and Dornhoffer 2002) and good experience with hydroxyapatite ceramics (Jahn 1992, Grote 1998), use of PLA/bioglass- or PLA/hydroxyapatite composites (Blaker et al. 2003, Hasegawa et al. 2007) for bone tissue engineering in the posterior wall and mastoidectomy cavity appears to have interesting potential. Because bioglass or hydroxyapatite alone is relatively difficult to mold into complex structures, the combination of PLA and ceramics would better meet this demand.

6.3 CONE-BEAM CT STUDIES (IV, V)

The main goals of Study IV were to evaluate the diagnostic accuracy of CBCT in imaging the middle ear structures and to compare the results with those from multislice helical CT. The CBCT equipment (3D Accuitomo) was designed for dental imaging, but was considered to be adequate for this pilot study. The helical CT (Aquilion) and the algorithm were routinely employed in the department in otologic imaging. Cadaver temporal bones were successfully imaged with both modalities, and according to the scaled evaluation of the images, there proved to be no significant differences in the precision of the methods in this setting. The estimated effective radiation dose of the CBCT was nearly 50-fold less than that calculated for the helical CT. The CNR—a generally accepted instrument for the assessment of the image quality (Siewerdsen et al. 2006)—was more than 50% lower in CBCT than in multislice helical CT, but still adequate for this diagnostic task.

The aim of Study V was to test the applicability of CBCT to the imaging of postoperative ear and middle ear implants. In addition, the image qualities obtained with different imaging

protocols were objectively compared by comparison of the CNRs calculated for the phantom images. The best CNRs of the phantom images were achieved with the highest tube current and voltage. However, the quality of bone images was graded as at least satisfactory with all the protocols. Furthermore, the protocol of values 2 mA/70 kVp produces the lowest radiation exposure, and it was used in Study IV with good results. These facts may support use of this protocol in prospective clinical pilot studies on otologic CBCT, although Dalchow et al. (2006b) used 8 mA/80 kVp when imaging patients with conductive hearing loss. As in Study IV, CBCT proved accurate in showing middle ear structures at a diagnostic level. Furthermore, visualization of middle ear implants was exact and in accordance with the procedures performed. Dislocation as well as the normal position of the piston prosthesis were detectable and locations of the titanium PORPs clearly visible.

Our findings on the diagnostic quality attained with CBCT support those of Dalchow et al. (2006a,b), who considered CBCT very accurate in showing anatomical details and the positions of ossicular replacement prostheses and of a cochlear implant. Thus, CBCT may be considered an alternative for helical CT in otologic imaging. Due to the limited FOV of the CBCT used, part of the mastoid was cut off the images. This clear disadvantage can be eliminated by enlarging the FOV sufficiently; this is enabled by current devices (Araki et al. 2004, Robinson et al. 2005) allowing imaging of the whole temporal bone area. Greater FOV also leads to increased irradiation required, however. In addition, with CBCT, only one ear can be examined at a time; consequently, when bilateral imaging is necessary, radiation dose doubles. Furthermore, differences appeared between the scan techniques and imaging protocols of the CBCT and the helical CT. Consequently, an exact and ultimate comparison of radiation doses directly applicable to clinical practice cannot be made on the basis of Study IV, although the mathematical comparison yielded a great difference between the doses of CBCT and helical CT. Low-dose settings in multislice helical CT can substantially reduce radiation dose, and in dental imaging the differences between the doses of CBCT and low-dose multislice CT have been relatively small (Cohnen et al. 2002, Suomalainen et al. 2008). However, with low-dose settings, the quality of the images also decreases, preventing soft-tissue differentiation and visualization of some sub-millimeter structures at diagnostic level.

When the skull of an actual patient is imaged instead of a cadaver temporal bone, between X-ray source and detector there lies more absorbent material out of the FOV. This causes a potential increase in the appearance of image artifacts and a decrease in low-contrast

resolution, due to beam hardening and X-ray scattering. In multislice helical CT, the attenuating structures of the patient's head are included in the scan FOV, which is a clear advantage of multislice CT over CBCT, when diagnostic resolution of soft tissues is required. In addition, the lower CBCT radiation dose leads to greater image noise and thus poorer low-contrast resolution (Robinson et al. 2005). However, the latest advances in CBCT technology have introduced new techniques and software algorithms for X-ray scatter estimation and correction, and for improving CNR and low-contrast resolution (Gomi et al. 2006, Siewerdsen et al. 2006, Tu et al. 2006, Graham et al. 2007). On the other hand, in imaging the middle and inner ear, visualization of small bony structures and cavities is most essential, and this requirement is well accomplished by CBCT—according to some reports even better than by multislice CT (Hashimoto et al. 2003, 2007, Sukovic 2003, Winter et al. 2005, Suomalainen et al. 2008). Furthermore, advantages for CBCT in general include a lower level of metal artifacts in images, and smaller, lower-priced, mobile equipment than for conventional CT (Scarfe et al. 2006).

Applying CBCT to clinical otological imaging requires a scanner model with a FOV sufficient for imaging of the whole temporal bone. Regardless of whether the patient is sitting or supine when imaged, the position and support of the patient's head must be correct. Optimal scan protocols for otological CBCT are vital, and also specified clinical indications for the examination. Furthermore, further comparable data on radiation doses of different CT modalities is essential.

In summary, based on the pilot studies conducted, justification exists for clinical studies on CBCT in otologic imaging. More research in this field is necessary to apply otologic CBCT to clinical practice.

7
CONCLUSIONS

There proved to be no more adherence of *Staphylococcous aureus* and *Pseudomonas aeruginosa* to PLGA than to silicone and titanium in vitro, indicating that the PLGA is an implant material as safe as silicone and titanium in this respect. Albumin coating significantly inhibited the adherence of these bacteria to PLGA, silicone, and titanium, suggesting that this method may be useful in implant surgery in specified situations for prevention of postoperative infections and improvement of implant biocompatibility.

PLGA showed good biocompatibility in the chinchilla middle ear within the 6-month follow-up, causing only a mild inflammatory response in the middle ear mucosa without signs of toxicity to the inner ear. No evident differences emerged in the biocompatibility of two different PLGA materials. Based on these results, prospective human studies on PLGA in ear surgery can be encouraged.

Limited cone-beam CT was at least as accurate as multislice helical CT in showing clinically important landmarks in the temporal bone. Positions of middle ear implants in relation to surrounding structures could be reliably evaluated with CBCT. In these images, PLGA appeared X-ray negative. The estimated effective radiation dose of CBCT was essentially lower than that of helical CT. Such findings support the implementation of prospective human studies on otologic CBCT for specifying indications and settings for clinical practice.

ACKNOWLEDGEMENTS

This study was carried out at the Department of Otorhinolaryngology, Helsinki University Central Hospital and Biomedicum, Helsinki, Finland. I want to express my deepest gratitude to all those who contributed to emergence of the thesis, especially to:

Professors Pekka Karma, Anne Pitkäranta, and Jukka Ylikoski, Docents Hans Ramsay and Heikki Rihkanen for providing excellent facilities for the study.

My supervisor Docent Jussi Jero for providing outstanding facilities, continuous support, and interesting research. Your clinical experience combined with your admirable creativeness in scientific thinking and work has been the driving force throughout this project. Your guidance, optimism, understanding, and encouragement have been invaluable and made this study possible.

My supervisor and long-time friend Docent Antti Aarnisalo for enjoyable cooperation and friendship throughout the past 18 years. We have known each other since early careless (and legendary) student times in medical school when we were playing and having a good time in "the" medical orchestra Valkotakit. On the way, we also served together as ENT residents at Jorvi Hospital. It has always been a privilege to work with you. Your endless enthusiasm and energy, good sense of humor, astonishing ability to manage a hundred things at the same time, and collegial, friendly attitude in clinical as well as in scientific work, have many times helped me to get on. Without your scientific and clinical experience, help and advice, encouraging and active touch for this study, this thesis would never have been completed. Thank you!

The reviewers of this work, Docents Jyrki Törnwall and Juha-Pekka Vasama, for your valuable comments and advice, and Dr. Carol Norris for your first-class language edit and professional courses with cozy atmosphere, and for bracing philosophical chats through e-mail regardless of time of day.

And to

Professor Antti Sukura for fruitful cooperation and for providing excellent facilities during the animal study in the Department of Basic Veterinary Sciences, and Docent Pentti Kuusela for sharing your vast knowledge in bacteriology and for providing exquisite facilities for the bacteriological studies in the Division of Clinical Microbiology in Haartman Institute.

My other co-authors, Dr. Teemu Kinnari, Professor Yrjö Konttinen, Dr. Soraya Robinson, Docent Mika Kortesniemi, Yvonne Käser, Laura Pietola, and Dr. Anni Suomalainen, for elegant cooperation. I want to thank particularly Teemu Kinnari for your indispensable, unselfish help and advice in bacteriological studies, and Mika Kortesniemi for offering time and making the effort for skillful completion of the radiological studies.

Sirke Haaka and Kati Meronen for your invaluable assistance with the animals and Eila Ketolainen for your skillful assistance in the lab.

Docent Henrik Malmberg, a great person and otorhinolaryngologist with huge clinical and scientific experience, under the guidance of whom I did my advanced special studies to graduate from the medical school as well as my early scientific publications. In addition to guiding me into the world of science, you were an excellent, patient teacher during my years of residency in Helsinki University Central Hospital and always there when I needed your help in the operating room. I am deeply indebted to you for everything.

Docent Heikki Rihkanen, an excellent educator, for forbearingly teaching me and sharing your vast knowledge in clinical and operative otorhinolaryngology during my residency in Jorvi Hospital, and for encouragement, understanding, and friendliness that were extremely important to me at that time.

Dr. Juha Silvola for providing me brilliant working facilities and teaching me ENT surgery, ear surgery in particular, during my residency in Päijät-Häme Central Hospital.

Drs. Jyrki Kaukonen and Samuli Suutarla for pleasant and smooth cooperation during our times of busy chief residency in Helsinki University Central Hospital.

All my colleagues and other personnel I have worked with in the Department of Otorhinolaryngology of different hospitals or in the enterprise sector for a warm and encouraging atmosphere that has been essential in keeping up my spirit for ENT.

All my friends outside the clinic and laboratory, especially Pasi, Max, Kapa, Panu, Ilu, and Aki for your friendship and the great times we have spent together. I owe special thanks to the one and only medical orchestra Valkotakit, a living legend, for unforgettable moments and cheering up my life outside medicine.

My mother Rita and my father Jari for your love and support throughout my life.
My sisters Anna, Liisa, and Maria, and my brother Risto, my best friends, for always having been there.

My parents-in-law, Leena and Pekka, my sister-in-law Elina, and my brother-in-law Mikko for your help and support.

The dearest persons in my life: my wife Hanna for your help, patience, support, understanding, and endless love; our wonderful children Juho, Ida, and Joel for making me happy, for filling our days with joy and love, and for confirming my idea of what is most important in life. Special thanks to our youngest child Joel for speeding up the completion of this thesis by being born.

This study was financially supported by Biomedicum Helsinki Foundation, the Finnish Medical Foundation, Instrumentarium Scientific Foundation, the Paulo Foundation, the Otologic Research Foundation, and a special governmental subsidy for health sciences research awarded by Helsinki University Central Hospital.

Nurmijärvi, May 2008

Lauri Peltonen

REFERENCES

Aimi K. Role of the tympanic ring in the pathogenesis of congenital cholesteatoma. Laryngoscope 93(9): 1140-1146, 1983.

Aitasalo K, Kinnunen I, Palmgren J, Varpula M. Repair of orbital floor fractures with bioactive glass implants. J Oral Maxillofac Surg 59: 1390-1395, 2001.

Al-Sukhun J, Törnwall J, Lindqvist C, Kontio R. Bioresorbable poly-L/DL-lactide (P[L/DL]LA 70/30) plates are reliable for repairing large inferior orbital wall bony defects: a pilot study. J Oral Maxillofac Surg 64(1): 47-55, 2006.

Amoils CP, Jackler RK, Milczuk H, Kelly KE, Cao K. An animal model of chronic tympanic membrane perforation. Otolaryngol Head Neck Surg 106(1): 47-55, 1992.

Al Anazy FH. Iatrogenic cholesteatoma in children with OME in a training program. Int J Pediatr Otorhinolaryngol 70: 1683-1686, 2006.

al-Khaffaf H, Charlesworth D. Albumin-coated vascular prostheses: a five-year follow-up. J Vasc Surg 23(4): 686-690, 1996.

An YH, Stuart GW, McDowell SJ, McDaniel SE, Kang Q, Friedman RJ. Prevention of bacterial adherence to implant surfaces with a crosslinked albumin coating *in vitro*. J Orthop Res 14(5): 846-849, 1996.

An YH, Bradley J, Powers DL, Friedman RJ. The prevention of prosthetic infection using a cross-linked albumin coating in a rabbit model. J Bone Joint Surg Br. 79(5): 816-819, 1997.

An YH, Friedman RJ. Concise review of mechanisms of bacterial adhesion to biomaterial surfaces. J Biomed Mater Res (Appl Biomater) 43(3): 338-348, 1998.

Arai Y, Tammisalo E, Iwai K, Hashimoto K, Shinoda K. Development of a compact computed tomographic apparatus for dental use. Dentomaxillofac Radiol 28(4): 245-248, 1999.

Araki K, Maki K, Seki K, Sakamaki K, Harata Y, Sakaino R, Okano T, Seo K. Characteristics of a newly developed dentomaxillofacial X-ray cone beam CT scanner (CB MercuRay™): system configuration and physical properties. Dentomaxillofac Radiol 33: 51-59, 2004.

Arguedas A, Loaiza C, Herrera JF, Mohs E. Antimicrobial therapy for children with chronic suppurative otitis media without cholesteatoma. Pediatr Infect Dis J 13(10): 878-882, 1994.

Aslam MA, Ahmed Z, Azim R. Microbiology and drug sensitivity patterns of chronic suppurative otitis media. J Coll Physicians Surg Pak 14(8): 459-61, 2004.

Baek C-H, Ko Y-J. Characteristics of tissue-engineered cartilage on macroporous biodegradable PLGA scaffold. Laryngoscope 116: 1829-1834, 2006.

Bala I, Hariharan S, Kumar MN. PLGA nanoparticles in drug delivery: the state of the art. Crit Rev Ther Drug Carrier Syst 21(5): 387-422.

Barth E, Myrvik QM, Wagner W, Gristina AG. *In vitro* and in *vivo* comparative colonization of *Staphylococcus aureus* and *Staphylococcus epidermidis* on orthopedic implant materials. Biomaterials 10(5): 325-328, 1989.

Bayles KW. The biological role of death and lysis in biofilm development. Nat Rev Mcrobiol 5(9): 721-726, 2007.

Biedlingmaier JF, Samaranayake R, Whelan P. Resistance to biofilm formation on otologic implant materials. Otolaryngol Head Neck Surg 118: 444-451, 1998.

Black B. Mastoidectomy elimination. Laryngoscope 105(12 Pt Suppl 76): 1-30, 1995.

Black B. Mastoidectomy elimination: Obliterate, reconstruct, or ablate? Am J Otol 19: 551-557, 1998.

Blake FA, Blessmann M, Pohlenz P, Heiland M. A new imaging modality for intraoperative evaluation of sinus floor augmentation. Int J Oral Maxillofac Surg 37(2): 183-185, 2007

Blaker JJ, Gough JE, Maquet V, Notingher I, Boccaccini AR. *In vitro* evaluation of novel bioactive composites based on Bioglass®-filled polylactide foams for bone tissue engineering scaffolds. J Biomed Mater Res 67A: 1401-1411, 2003.

Blindt R, Hoffmeister KM, Bienert H, Pfannschmitt, Bartsch G, Thiessen H, Klee D, Vom Dahl J. Development of a new biodegradable intravascular polymer stent with simultaneous incorporation of bioactive substances. Int J Artif Organs 22(12): 843-853, 1999.

Bluestone CD, Klein JO. Otitis media in infants and children; 2nd ed., WB Saunders Company; Philadelphia, USA, 1995: pp. 1-3, 18-29, 204-215, 250-270.

Boeddinghaus R, Whyte A. Current concepts in maxillofacial imaging. Eur J Radiol 2007, *Epub ahead of print*.

Brackmann DE, Shelton C, Arriaga MA. Otologic surgery; 2nd ed., W.B. Saunders Company, Philadelphia, USA, 2001: pp. 68-81, 88-215.

Brook I. Role of anaerobic bacteria in chronic otitis media and cholesteatoma. Int J Pediatr Otorhinolaryngol 31(2-3): 153-157, 1995.

Brown MR, Allison DG, Gilbert P. Resistance of bacterial biofilms to antibiotics: a growth-related effect? J Antimicrob Chemother 22(6): 777-780, 1988.

Böstman OM, Pihlajamäki HK, Partio EK, Rokkanen PU. Clinical biocompatibility and degradation of polylevolactide screws in the ankle. Clin Orthop Relat Res 320: 101-109, 1995.

Buckingham RA. Cholesteatoma and chronic otitis media following middle ear intubation. Laryngoscope 91(9 Pt 1): 1450-1456, 1981.

Böstman OM, Pihlajamäki HK. Adverse tissue reactions to bioabsorbable fixation devices. Clin Orthop Relat Res 371: 216-227, 2000.

Caldemeyer KS, Sandrasegaran K, Shinaver CN, Mathews VP, Smith RR, Kopecky KK. Temporal bone: comparison of isotropic helical CT and conventional direct axial and coronal CT. Am J Roentgenol 172(6): 1675-1682, 1999.

Casselman JW. Temporal bone imaging. Neuroimaging Clin N Am 6(2): 265-289, 1996.

Chao WY, Tseng HZ, Chang SJ. Eustachian tube dysfunction in the pathogenesis of cholesteatoma: clinical considerations. J Otolaryngol 25(5): 334-338, 1996.

Chen J, Morin O, Aubin M, Bucci MK, Chuang CF, Pouliot J. Dose-guided radiation therapy with megavoltage cone-beam CT. Br J Radiol 79: 587-598, 2006.

Chen YT, Wang HL, Lopatin DE, O´Neal R, MacNeil RL. Bacterial adherence to guided tissue regeneration barrier membranes exposed to the oral environment. J Periodontol 68(2): 172-179, 1997.

Cho PS, Johnson RH, Griffin TW. Cone-beam CT for radiotherapy applications. Phys Med Biol 40(11): 1863-1883, 1995.

Cho S, Bian J, Pelizzari CA, Chen CT, He TC, Pan X. Region-of-interest image reconstruction in circular cone-beam micro-CT. Med Phys 34(12): 4923-4933, 2007.

Chole RA. Squamous metaplasia of the middle ear mucosa during vitamin A deprivation. Otolaryngol Head Neck Surg 87(6): 837-844, 1979.

Chole RA, Hubbell RN. Antimicrobial activity of silastic tympanostomy tubes impregnated with silver oxide. A double-blind randomized multicenter trial. Arch Otolaryngol Head Neck Surg 121: 562-565, 1995.

Chole RA, Faddis BT. Evidence for microbial biofilms in cholesteatomas. Arch Otolaryngol Head Neck Surg 128(10): 1129-1133, 2002.

Chole RA, Faddis BT. Anatomical evidence of microbial biofilms in tonsillar tissues. Arch Otolaryngol Head Neck Surg 129: 634-636, 2003.

Chu CC, Williams DF. Effects of physical configuration and chemical structure of suture materials on bacterial adhesion. A possible link to wound infection. Am J Surg 147(2): 197-204, 1984.

Cohnen M, Kemper J, Möbes O, Pawelzik J, Mödder U. Radiation dose in dental radiology. Eur Radiol 12: 634-637, 2002.

Cormio L, La Forgia P, Siitonen A, Ruutu M, Törmälä P, Talja M. Immersion in antibiotic solution prevents bacterial adhesion onto biodegradable prostatic stents. Br J Urol 79(3): 409-413, 1997.

Costerton JW, Lewandowski Z, Caldwell DE, Korber DR, Lappin-Scott HM. Microbial biofilms. Annu Rev Microbiol 49: 711-745, 1995.

Costerton JW, Stewart PS, Greenberg EP. Bacterial biofilms: a common cause of persistent infections. Science 284: 1318-1322, 1999.

Cruz OL, Kasse CA, Leonhart FD. Efficacy of surgical treatment of chronic otitis media. Otolaryngol Head Neck Surg 128: 263-266, 2003.

Cummings CW, Fredrickson JM, Harker LA, Krause CJ, Schuller DE, Richardson MA. Otolaryngology - Head and neck surgery; 3rd ed., Mosby – Year book, Inc., St. Louis, USA, 1998: pp. 25-83, 3027-3075.

Cunliffe D, Smart CA, Alexander C, Vulfson EN. Bacterial adhesion at synthetic surfaces. Appl Environ Microbiol 65(11): 4995-5002, 1999.

Curtin HD. Superior semicircular canal dehiscence syndrome and multi-detector row CT. Radiology 226: 312-314, 2003.

Czerny C, Gstoettner W, Franz P, Baumgartner WD, Imhof H. CT and MR imaging of acquired abnormalities of the inner ear and cerebellopontine angle. Eur J Radiol 40: 105-112, 2001.

da Costa SS, Paparella MM, Schachern PA, Yoon TH, Kimberley BP. Temporal bone histopathology in chronically infected ears with intact and perforated tympanic membranes. Laryngoscope 102(11): 1229-1236, 1992.

Dalchow CV, Grün D, Stupp HF. Reconstruction of the ossicular chain with titanium implants. Otolaryngol Head Neck Surg 125(6): 628-630, 2001.

Dalchow CV, Weber AL, Yanagihara N, Bien S, Werner JA. Digital volume tomography: radiological examinations of the temporal bone. AJR 186: 416-423, 2006a.

Dalchow CV, Weber AL, Bien S, Yanagihara N, Werner JA. Value of digital volume tomography in patients with conductive hearing loss. Eur Arch Otorhinolaryngol 263: 92-99, 2006b.

Daly MJ, Siewerdsen JH, Moseley DJ, Jaffray DA, Irish JC. Intraoperative cone-beam CT for guidance of head and neck surgery: assessment of dose and image quality using a C-arm prototype. Med Phys 33(10): 3767-3780, 2006.

Darouiche RO. Treatment of infections associated with surgical implants. New Engl J Med 350: 1422-1429, 2004.

Darouiche RO. Antimicrobial coating of devices for prevention of infection: principles and protection. Int J Artif Organs 30(9): 820-827, 2007.

Darouiche RO, Mansouri MD, Zakarevicz D, Alsharif A, Landon GC. In vivo efficacy of antimicrobial-coated devices. J Bone Joint Surg Am 89(4): 792-797, 2007.

De Foer B, Vercruysse J-P, Bernaerts A, Maes J, Deckers F, Michiels J, Somers T, Pouillon M, Offeciers E, Casselman JW. The value of single-shot turbo spin-echo diffusion-weighted MR imaging in the detection of middle ear cholesteatoma. Neuroradiol 49(10): 841-848, 2007.

Dietrich L, Jetter S, Tücking T, Nill S, Oelfke U. Linac-integrated 4D cone beam CT: first experimental results. Phys Med Biol 51(11): 2939-2952, 2006.

Ding GX, Duggan DM, Coffey CW, Deeley M, Hallahan DE, Cmelak A, Malcolm A. A study on adaptive IMRT treatment planning using kV cone-beam CT. Radiother Oncol 85(1): 116-125, 2007.

Downey TJ, Champeaux AL, Silva AB. AlloDerm tympanoplasty of tympanic membrane perforations. Am J Otolaryngol 24(1): 6-13, 2003.

Dubrulle F, Souillard R, Chechin D, Vaneecloo FM, Desaulty A, Vincent C. Diffusion-weighted MR imaging sequence in the detection of postoperative recurrent cholesteatoma. Radiology 238(2): 604-610, 2006.

Dufresne AM, Lafreniere D. Soft tissue response in the rabbit larynx following implantation of Lactosorb (PLA/PGA copolymer) prosthesis for medialization laryngoplasty. J Voice 14(3): 387-397, 2000.

El-Bitar MA, Choi SS, Emamian SA, Vezina LG. Congenital middle ear cholesteatoma: need for early recognition – role of computed tomography scan. Int J Pediatr Otorhinolaryngol 67(3): 231-235, 2003.

Elsheikh EL, Abaas S, Wretlind B. Adherence of Pseudomonas aeruginosa to tracheal epithelial cells of mink. Studies on bacterial hydrophobicity and elastase production. Acta Pathol Microbiol Immunol Scand [B] 93(6): 417-422, 1985.

Emery BE, Dixit R, Formby C, Biedlingmaier JF. The resistance of maxillofacial reconstruction plates to biofilm formation in vitro. Laryngoscope 113: 1977-1982, 2003.

Eppley BL, Reilly M. Degradation characteristics of PLLA-PGA bone fixation devices. J Craniofac Surg 8(2): 116-120, 1997.

Erstad BL. Viral infectivity of albumin and plasma protein fraction. Pharmacotherapy 16(6): 996-1001, 1996.

Everaert EP, Mahieu HF, Wong Chung RP, Verkerke GJ, van der Mei HC, Busscher HJ. A new method for in vivo evaluation of biofilms on surface-modified silicone rubber voice prostheses. Eur Arch Otorhinolaryngol 254(6): 261-263, 1997.

Feenstra L, Kohn FE, Feyen J. The concept of an artificial tympanic membrane. Clin Otolaryngol 9: 215-220, 1984.

Fisch U, May J, Linder T, Naumann IC. A new L-shaped titanium prosthesis for total reconstruction of the ossicular chain. Otol Neurotol 25: 891-902, 2004.

Fliss DM, Dagan R, Houri Z, Leiberman A. Medical management of chronic suppurative otitis media without cholesteatoma in children. J Pediatr 116(6): 991-996, 1990.

Fliss DM, Dagan R, Meidan N, Leiberman A. Aerobic bacteriology of chronic suppurative otitis media without cholesteatoma in children. Ann Otol Rhinol Laryngol 101(10): 866-869, 1992.

Giardino R, Fini M, Aldini NN, Giavaresi G, Rocca M. Polylactide bioabsorbable polymers for guided tissue regeneration. J Trauma 47(2): 303-308, 1999.

Giardino R, Aldini NN, Fini M, Tanzi MC, Faré S, Draghi L, Carpi A, Nicolini A, Giavaresi G. Bioabsorbable scaffold for in situ bone regeneration. Biomed Pharmacother 60(8): 386-392, 2006.

Gogolewski S, Pineda L, Büsing CM. Bone regeneration in segmental defects with resorbable polymeric membranes: IV. Does the polymer chemical composition affect the healing process? Biomaterials 21: 2513-2520, 2000.

Gomi T, Koshida K, Miyati T. Development of a cone angle weighted three-dimensional image reconstruction algorithm to reduce cone-beam artefacts. Dentomaxillofac Radiol 35(6): 398-406, 2006.

Goycoolea MV, Muchow DC, Sirvio LM, Winandy RM. In search of missing links in otology. II. Development of an implantable middle ear drug delivery system: initial studies of sustained ampicillin release for the treatment of otitis media. Laryngoscope 101(7 Pt 1): 727-732, 1991.

Goycoolea MV, Muchow DC, Sirvio LM, Winandy RM, Canafax DM, Hueb M. Extended middle ear drug delivery. A new concept; a new device. Acta Otolaryngol Suppl 493: 119-126, 1992.

Goycoolea MV, Muchow DC. Sustained release of antimicrobials in the middle ear using a biodegradable support. Ann Otol Rhinol Laryngol Suppl 163: 46-48, 1994.

Graham SA, Moseley DJ, Siewerdsen JH, Jaffray DA. Compensators for dose and scatter management in cone-beam computed tomography. Med Phys 34(7): 2691-2703, 2007.

Gristina AG, Costerton JW. Bacterial adherence to biomaterials and tissue. The significance of its role in clinical sepsis. J Bone Joint Surg Am 67(2): 264-273, 1985.

Gristina AG, Hobgood CD, Webb LX, Myrvik QN. Adhesive colonization of biomaterials and antibiotic resistance. Biomaterials 8(6): 423-426, 1987.

Gristina AG. Biomaterial-centered infection: microbial adhesion versus tissue integration. Science 237(4822): 1588-1595, 1987.

Gross U, Strunz V. The interface of various glasses and glass ceramics with a bony implantation bed. J Biomed Mater Res 19(3): 251-271, 1985.

Grote JJ. Reconstruction of the middle ear with hydroxylapatite implants: long-term results. Ann Otol Rhinol Laryngol Suppl 144: 12-16, 1990.

Grote JJ. Results of cavity reconstruction with hydroxyapatite implants after 15 years. Am J Otol 19(5): 565-568, 1998.

Guckenberger M, Meyer J, Wilbert J, Baier K, Mueller G, Wulf J, Flentje M. Cone-beam CT based image-guidance for extracranial stereotactic radiotherapy of intrapulmonary tumors. Acta Oncol 45(7): 897-906, 2006.

Guerrero ME, Jacobs R, Loubele M, Schutyser F, Suetens P, van Steenberghe D. State-of-the-art on cone beam CT imaging for preoperative planning of implant placement. Clin Oral Investig 10(1): 1-7, 2006.

Gupta R, Bartling SH, Basu SK, Ross WR, Becker H, Pfoh A, Brady T, Curtin HD. Experimental flat-panel high-spatial-resolution volume CT of the temporal bone. Am J Neuroradiol 25: 1417-1424, 2004.

Hafidh MA, Keogh I, Walsh RM, Walsh M, Rawluk D. Otogenic intracranial complications. A 7-year retrospective review. Am J Otolaryngol 27(6): 390-395, 2006.

Hall-Stoodley L, Hu FZ, Gieseke A, Nistico L, Nguyen D, Hayes J, Forbes M, Greenberg DP, Dice B, Burrows A, Wackym PA, Stoodley P, Post JC, Ehrlich GD, Kerschner JE. Direct detection of bacterial biofilms on the middle-ear mucosa of children with chronic otitis media. JAMA 296(2): 202-211, 2006.

Hasegawa S, Tamura J, Neo M, Goto K, Shikinami Y, Saito M, Kita M, Nakamura T. In vivo evaluation of a porous hydroxyapatite/poly-DL-lactide composite for bone tissue engineering. J Biomed Mater Res 81A: 930-938, 2007.

Hashimoto K, Arai Y, Iwai K, Araki M, Kawashima S, Terekado M. A comparison of a new limited cone beam computed tomography machine for dental use with a multidetector row helical CT machine. Oral Surg Oral Med Oral Pathol Oral Radiol Endod 95: 371-377, 2003.

Hashimoto K, Kawashima S, Kameoka S, Akiyama Y, Honjoya T, Ejima K, Sawada K. Comparison of image validity between cone beam computed tomography for dental use and multidetector row helical computed tomography. Dentomaxillofac Radiol 36(8): 465-471, 2007.

Hench LL, Ethridge EC. Biomaterials, an interfacial approach. Academic Press, New York, USA, 1982.

Heiland M, Pohlenz P, Blessmann M, Habermann CR, Oesterhelweg L, Begemann PC, Schmidgunst C, Blake FA, Püschel K, Schmelze R, Schulze D. Cervical soft tissue imaging using a mobile CBCT scanner with a flat panel detector in comparison with corresponding CT and MRI data sets. Oral Surg Oral Med Oral Pathol Oral Radiol Endod 104: 814-820, 2007.

Heiland M, Pohlenz P, Blessmann M, Werle H, Fraedrich M, Schmelzle R, Blake FA. Navigated implantation after microsurgical bone transfer using intraoperatively acquired cone-beam computed tomography data sets. Int J Oral Maxillofac Surg 37: 70-75, 2008.

Hietala, EM, Salminen US, Ståhls A, Välimaa T, Maasilta P, Törmälä P, Nieminen MS, Harjula AL. Biodegradation of the copolymeric polylactide stent. Long-term follow-up in a rabbit aorta model. J Vasc Res 38(4): 361-369, 2001.

Hintze H, Wiese M, Wenzel A. Cone beam CT and conventional tomography for the detection of morphological temporomandibular joint changes. Dentomaxillofac Radiol 36(4): 192-197, 2007.

Hirota S, Nakao N, Yamamoto S, Kobayashi K, Maeda H, Ishikura R, Miura K, Sakamoto K, Ueda K, Baba R. Cone-beam CT with flat-panel-detector digital angiography system: early experience in abdominal interventional procedures. Cardiovasc Intervent Radiol 29(6): 1034-1038, 2006.

Hogt AH, Dankert J, Feijen J. Adhesion of *Staphylococcus epidermidis* and *Staphylococcus saprophyticus* to a hydrophobic biomaterial. J Gen Microbiol 131(9): 2485-2491, 1985.

Hostacká A, Ciznár I, Slobodníkova L, Kotulová D. Clinical pseudomonas aeruginosa: potential factors of pathogenicity and resistance to antimicrobials. Folia Microbiol 51(6): 633-638, 2006.

Hyde JA, Chinn JA, Phillips RE Jr. Polymer heart valves. J Heart Valve Dis 8(3): 331-339, 1999.

Hüttenbrink KB. Surgical treatment of chronic otitis media. III: Middle ear reconstruction. HNO 42(11): 701-718, 1994.

Indudharan R, Haq JA, Aiyar S. Antibiotics in chronic suppurative otitis media: a bacteriologic study. Ann Otol Rhinol Laryngol 108(5): 440-445, 1999.

Isotalo T, Alarakkola E, Talja M, Tammela TL, Välimaa T, Törmälä P. Biocompatibility testing of a new bioabsorbable x-ray positive SR-PLA 96/4 urethral stent. J Urol 162(5): 1764-1767, 1999.

Ito K, Gomi Y, Sato S, Arai Y, Shinoda K. Clinical application of a new compact CT system to assess 3-D images for the preoperative treatment planning of implants in the posterior mandible. A case report. Clin Oral Impl Res 12: 539-542, 2001.

Jackler RK, Parker DA. Radiographic differential diagnosis of petrous apex lesions. Am J Otol 13(6): 561-574, 1992.

Jahn AF. Experimental applications of porous (coralline) hydroxylapatite in middle ear and mastoid reconstruction. Laryngoscope 102: 289-299, 1992.

Jain R, Gandhi D, Gujar S, Mukherji SK. Case 67: persistent stapedial artery. Radiology 230: 413-416, 2004.

Jung TT, Park SK. Reconstruction of mastoidectomy defect with titanium mesh. Acta Otolaryngol 124(4): 440-442, 2004.

Kakeda S, Korogi Y, Miyaguni Y, Moriya J, Ohnari N, Oda N, Nishino K, Miyamoto W. A cone-beam volume CT using a 3D angiography system with a flat panel detector of direct conversion type: usefulness for superselective intra-arterial chemotherapy for head and neck tumors. Am J Neuroradiol 28(9): 1783-1788, 2007a.

Kakeda S, Korogi Y, Ohnari N, Moriya J, Oda N, Nishino K, Miyamoto W. Usefulness of cone-beam volume CT with flat panel detectors in conjunction with catheter angiography for transcatheter arterial embolization. J Vasc Interv Radiol 18(12): 1508-1516, 2007b.

Kallela I, Tulamo RM, Hietanen J, Pohjonen T, Suuronen R, Lindqvist C. Fixation of mandibular body osteotomies using biodegradable amorphous self-reinforced (70L:30DL) polylactide or metal lag screws: an experimental study in sheep. J Craniomaxillofac Surg 27(2): 124-133, 1999.

Karakeçili AG, Gümüşderelioğlu M. Comparison of bacterial and tissue cell initial adhesion on hydrophilic/hydrophobic biomaterials. J Biomater Sci Polym Ed 13(2): 185-196, 2002.

Karmody CS, Byahatti SV, Blevins N, Valtonen H, Northrop C. The origin of congenital cholesteatoma. Am J Otol 19(3): 292-297, 1998.

Katsikogianni M, Missirlis YF. Concise review of mechanisms of bacterial adhesion to biomaterials and of techniques used in estimating bacteria-material interactions. Eur Cell Mater 8: 37-57, 2004.

Kazahaya K, Potsic WP. Congenital cholesteatoma. Curr Opin Otolaryngol Head Neck Surg 12(5): 398-403, 2004.

Keane PF, Bonner MC, Johnston SR, Zafar A, Gorman SP. Characterization of biofilm and encrustation on ureteric stents in vivo. Br J Urol 73(6): 687-691, 1994.

Kenna MA, Bluestone CD, Reilly JS, Lusk RP. Medical management of chronic suppurative otitis media without cholesteatoma in children. Laryngoscope 96(2): 146-151, 1986.

Keogh JR, Eaton JW. Albumin binding surfaces for biomaterials. J Lab Clin Med 124(4): 537-545, 1994.

Ketelslagers K, Somers T, De Foer B, Zarowski A, Offeciers E. Results, hearing rehabilitation, and follow-up with magnetic resonance imaging after tympanomastoid exentration, obliteration, and external canal overclosure for severe chronic otitis media. Ann Otol Rhinol Laryngol 116(9): 705-711, 2007.

Khoury A, Siewerdsen JH, Whyne CM, Daly MJ, Kreder HJ, Moseley DJ, Jaffray DA. Intraoperative cone-beam CT for image-guided tibial plateau fracture reduction. Comput Aided Surg 12(4): 195-207, 2007.

Kim HH, Battista RA, Kumar A, Wiet RJ. Should ossicular reconstruction be staged following tympanomastoidectomy. Laryngoscope 116(1): 47-51, 2006.

Kinnari TJ, Salonen E-M, Jero J. New method for coating tympanostomy tubes to prevent tube occlusions. Int J Pediatr Otorhinolaryngol 58: 107-111, 2001.

Kinnari TJ, Salonen E-M, Jero J. Durability of the binding inhibition of albumin coating on tympanostomy tubes. Int J Pediatr Otorhinolaryngol 67: 157-164, 2003.

Kinnari TJ, Rihkanen H, Laine T, Salonen E-M, Jero J. Albumin-coated tympanostomy tubes: prospective, double-blind clinical study. Laryngoscope 114: 2038-2043, 2004.

Kinnari TJ, Jero J. Experimental and clinical experience of albumin coating of tympanostomy tubes. Otolaryngol Head Neck Surg 133: 596-600, 2005.

Kinnari TJ, Rihkanen H, Laine T, Salonen E-M, Jero J. Role of albumin coating of tympanostomy tubes: long-term clinical evaluation. Laryngoscope 117: 2213-2217, 2007.

Klein AM, Graham VL, Gulleth Y, Lafreniere D. Polyglycolic acid/poly-L-lactic acid copolymer use in laryngotracheal reconstruction: a rabbit model. Laryngoscope 115(4): 583-587, 2005.

Klingebiel R, Bauknecht HC, Freigang B, Kaschke O, Linke R, Meuschel-Werner S, Werbs M, Lehmann R. Multislice computed tomographic imaging in temporal bone dysplasia. Otol Neurotol 23(5): 715-722, 2002.

Kojic EM, Darouiche RO. Candida infections of medical devices. Clin Microbiol Rev 17(2): 255-267, 2004.

Kojima H, Miyazaki H, Shiwa M, Tanaka Y, Moriyama H. Molecular biological diagnosis of congenital and acquired cholesteatoma on the basis of differences in telomere length. Laryngoscope 111: 867-873, 2001.

Koltai PJ, Nelson M, Castellon RJ, Garabedian E-N, Triglia J-M, Roman S, Roger G. The natural history of congenital cholesteatoma. Arch Otolaryngol Head Neck Surg 128: 804-809, 2002.

Kontio R, Salo A, Suuronen R, Lindqvist C, Meurman JH, Virtanen I. Fibrous wound repair associated with biodegradable poly-L/D-lactide copolymer implants: study of the expression of tenascin and cellular fibronectin. J Mater Sci Mater Med 9(10): 603-609, 1998.

Kontio R, Ruuttila P, Lindroos L, Suuronen R, Salo A, Lindqvist C, Virtanen I, Konttinen YT. Biodegradable polydioxanone and poly(L/D)lactide implants: an experimental study on peri-implant tissue response. Int J Oral Maxillofac Surg 34: 766-776, 2005.

Korpela A, Aarnio P, Sariola H, Törmälä P, Harjula A. Comparison of tissue reactions in the tracheal mucosa surrounding a bioabsorbable and silicone airway stents. Ann Thorac Surg 66: 1772-1776, 1998.

Korpela A, Aarnio P, Sariola H, Törmälä P, Harjula A. Bioabsorbable self-reinforced poly-l-lactide, metallic, and silicone stents in the management of experimental tracheal stenosis. Chest 115: 490-495, 1999.

Kuusela P, Vartio T, Vuento M, Myhre EB. Attachment of staphylococci and streptococci on fibronectin, fibronectin fragments, and fibrinogen bound to a solild phase. Infect Immun 50(1): 77-81, 1985.

Kwon IK, Park KD, Choi SW, Lee SH, Lee EB, Na JS, Kim SH, Kim YH. Fibroblast culture on surface-modified poly(glycolide-co-epsilon-caprolactone) scaffold for soft tissue regeneration. J Biomater Sci Polym Ed 12(10): 1147-1160, 2001.

Kösling S, Bootz F. CT and MR imaging after middle ear surgery. Eur J Radiol 40: 113-118, 2001.

Landes CA, Ballon A, Roth C. In-patient versus in vitro degradation of P(L/DL)LA and PLGA. J Biomed Mater Res B Appl Biomater 76(2): 403-411, 2006a.

Landes CA, Ballon A, Roth C. Maxillary and mandibular osteosyntheses with PLGA and P(L/DL)LA implants: a 5-year inpatient biocompatibility and degradation experience. Plast Reconstr Surg 117: 2347-2360, 2006b.

Lazard DS, Roger G, Denoyelle F, Chauvin P, Garabédian E-N. Congenital cholesteatoma: risk factors for residual disease and retraction pockets – a report on 117 cases. Laryngoscope 117: 634-637, 2007.

Leatherman BD, Dornhoffer JL. Bioactive glass ceramic particles as an alternative for mastoid obliteration: results in an animal model. Otol Neurotol 23: 657-660, 2002.

Leskinen K, Jero J. Acute complications of otitis media in adults. Clin Otolaryngol 30(6): 511-516, 2005.

Lewandrowski KU, Gresser JD, Wiese DL, Trantolo DJ, Hasirci V. Tissue responses to molecularly reinforced polylactide-co-glycolide implants. J Biomater Sci Polym Ed 11(4): 401-414, 2000.

Li B, Logan BE. Bacterial adhesion to glass and metal-oxide surfaces. Colloids Surf B Biointerfaces 36(2): 81-90, 2004.

Lim SY, Mun GH, Hyon WS, Bang SI, Oh KS. The elevation of the reconstructed auricle with a temporoparietal fascial flap wrapping a resorbable plate. J Plast Reconstr Aesthet Surg 59(5): 505-509, 2006.

Linsenmaier U, Rock C, Euler E, Wirth S, Brandl R, Kotsianos D, Mutschler W, Pfeifer KJ. Three-dimensional CT with a modified C-arm image intensifier: feasibility. Radiology 224: 286-292, 2002.

Ludwick JJ, Rossmann SN, Johnson MM, Edmonds JL. The bacteriostatic properties of ear tubes made of absorbable polylactic acid. Int J Pediatr Otorhinolaryngol 70: 407-410, 2006.

Lumiaho J, Heino A, Pietiläinen T, Ala-Opas M, Talja M, Välimaa T, Törmälä P. The morphological , in situ effects of a self-reinforced bioabsorbable polylactide (SR-PLA 96) ureteric stent; an experimental study. J Urol 164(4): 1360-1363, 2000.

Lundeberg T. Prevention of catheter associated urinary tract infections by use of silver-impregnated catheters. Lancet 2: 1031, 1986.

Lynch AS, Robertson GT. Bacterial and fungal biofilm infections. Annu Rev Med 59: 1-14, 2008.

Machin K, Webb S. Cone-beam x-ray microtomography of small specimens. Phys Med Biol 39(10): 1639-1657, 1994.

MacKintosh EE, Patel JD, Marchant RE, Anderson JM. Effects of biomaterial surface chemistry on the adhesion and biofilm formation of *Staphylococcus epidermidis in vitro*. J Biomed Mater Res A 78(4): 836-842, 2006.

Mah JK, Danforth RA, Bumann A, Hatcher D. Radiation absorbed in maxillofacial imaging with a new dental computed tomography device. Oral Surg Oral Med Oral Pathol Oral Radiol Endod 96: 508-513, 2003.

Maroldi R, Farina D, Palvarini L, Marconi A, Gadola E, Menni K, Battaglia G. Computed tomography and magnetic resonance imaging of pathologic conditions of the middle ear. Eur J Radiol 40: 78-93, 2001.

Massey BL, Wen X, Rohr RL, Tresco PA, Dahlström L, Park AH. Resorption rate and biocompatibility characteristics of two polyester ventilation tubes in a guinea pig model. Otolaryngol Head Neck Surg 131: 921-925, 2004.

McAllister EW, Carey LC, Brady PG, Heller R, Kovacs SG. The role of polymeric surface smoothness of biliary stents in bacterial adherence, biofilm deposition, and stent occlusion. Gastrointest Endosc 39(3): 422-425, 1993.

Merchant RE. The cage implant system for determining in vivo biocompatibility of medical device materials. Fundam Appl Toxicol 13(2): 217-227, 1989.

Merritt K, Shafer JW, Brown SA. Implant site infection rates with porous and dense materials. J Biomed Mater Res 13(1): 101-108, 1979.

Migirov L. Computed tomographic versus surgical findings in complicated acute otomastoiditis. Ann Otol Rhinol Laryngol 112: 675-677, 2003.

Morin O, Gillis A, Chen J, Aubin M, Bucci MK, Roach M 3rd, Pouliot J. Megavoltage cone-beam CT: system description and clinical applications. Med Dosim 31(1): 51-61, 2006.

Morin O, Chen J, Aubin M, Gillis A, Aubry JF, Bose S, Chen H, Descovich M, Xia P, Pouliot J. Dose calculation using megavoltage cone-beam CT. Int J Radiat Oncol Biol Phys 67(4): 1201-1210, 2007.

Morris NS, Stickler DJ, McLean RJ. The development of bacterial biofilms on indwelling urethral catheters. World J Urol 17(6): 345-350, 1999.

Mozzo P, Procacci C, Tacconi A, Martini PT, Andreis IA. A new volumetric CT machine for dental imaging based on the cone-beam technique: preliminary results. Eur Radiol 8(9): 1558-1564, 1998.

Mukherjee P, Saunders N, Liu R, Fagan P. Long-term outcome of modified radical mastoidectomy. J Laryngol Otol 118(8): 612-616, 2004.

Multanen M, Talja M, Hallanvuo S, Siitonen A, Välimaa T, Tammela TL, Seppälä J, Törmälä P. Bacterial adherence to ofloxacin-blended polylactone-coated self-reinforced L-lactic acid polymer urological stents. BJU Int 86: 966-969, 2000a.

Multanen M, Talja M, Hallanvuo S, Siitonen A, Välimaa T, Tammela T, Seppälä J, Törmälä P. Bacterial adherence to silver nitrate coated poly-l-lactic acid urological stents in vitro. Urol Res 28: 327-331, 2000b.

Multanen M, Tammela TL, Laurila M, Seppälä J, Välimaa T, Törmälä P, Talja M. Biocompatibility, encrustation and biodegradation of ofloxacine and silver nitrate coated poly-L-lactic acid stents in rabbit urethra. Urol Res 30(4): 227-232, 2002.

Nalwa SS, Hartig GK, Connor NP, Warner T, Thielman MJ. Evaluation of poly-l-lactic acid and polyglycolic acid resorbable stents for repair of tracheomalacia in a porcine model. Ann Otol Rhinol Laryngol 110: 993-999, 2001.

Nelson M, Roger G, Koltai PJ, Garabedian E-N, Triglia J-M, Roman S, Castellon RJ, Hammel JP. Congenital cholesteatoma. Arch Otolaryngol Head Neck Surg 128: 810-814, 2002.

Neumann A, Schultz-Coulon H-J, Jahnke K. Type III tympanoplasty applying the palisade cartilage technique: a study of 61 cases. Otol Neurotol 24: 33-37, 2003.

Nickenig HJ, Eitner S. Reliability of implant placement after virtual planning of implant positions using cone beam CT data and surgical (guide) templates. J Craniomaxillofac Surg 35(4-5): 207-211, 2007.

Niemelä SM, Ikäheimo I, Koskela M, Veiranto M, Suokas E, Törmälä P, Waris T, Ashammaki N, Syrjälä H. Ciprofloxacin-releasing bioabsorbable polymer is superior to titanium in preventing *Staphylococcus epidermidis* attachment and biofilm formation *in vitro*. J Biomed Mater Res Part B: Appl Biomater 76B: 8-14, 2006.

Nordström P, Pihlajamäki H, Toivonen T, Törmälä P, Rokkanen P. Tissue responses to polyglycolide and polylevolactide pins in osteotomized cancellous bone. Clin Orthop Relat Res 382: 247-257, 2001.

Olszewska E, Chodynicki S, Chyczewski L. Apoptosis in the pathogenesis of cholesteatoma in adults. Eur Arch Otorhinolaryngol 263: 409-413, 2006.

Packham MA, Evans G, Glynn MF, Mustard JF. The effect of plasma proteins on the interaction of platelets with glass surfaces. J Lab Clin Med 73: 686-697, 1969.

Palmer J, Flint S, Brooks J. Bacterial cell attachment, the beginning of a biofilm. J Ind Microbiol Biotechnol 34(9): 577-588, 2007.

Palva T. Mastoid obliteration. Acta Otolaryngol Suppl 360: 152-154, 1979.

Palva T, Mäkinen J. The meatally based musculoperiosteal flap in cavity obliteration. Arch Otolaryngol 105(7): 377-380, 1979.

Palva T. Surgical treatment of chronic middle ear disease. II. Canal wall up and canal wall down procedures. Acta Otolaryngol 104(5-6): 487-494, 1987a.

Palva T. Surgical treatment of chronic middle ear disease. 1. Myringoplasty and tympanoplasty. Acta Otolaryngol 104(3-4): 279-284, 1987b.

Palva T. The pathogenesis and treatment of cholesteatoma. Acta Otolaryngol 109(5-6): 323-330, 1990.

Palva T. Cholesteatoma surgery today. Clin Otolaryngol Allied Sci 18(4): 245-252, 1993.
Park TG. Degradation of poly(lactic-co-glycolic acid) microspheres: effect of copolymer composition. Biomaterials 16(15): 1123-1130, 1995.

Pawlowski KS, Wawro D, Roland PS. Bacterial biofilm formation on a human cochlear implant. Otol Neurotol 26: 972-975, 2005.

Peltola M, Suonpää J, Aitasalo K, Varpula M, Yli-Urpo A, Happonen R-P. Obliteration of the frontal sinus cavity with bioactive glass. Head Neck 20: 315-319, 1998.

Persaud R, Hajioff D, Trinidade A, Khemani S, Bhattacharyya MN, Papadimitriou N, Kalan A, Bhattacharyya AK. Evidence-based review of aetiopathogenic theories of congenital and acquired cholesteatoma. J Laryngol Otol 121(11): 1013-1019, 2007.

Petas A, Vuopio-Varkila J, Siitonen A, Välimaa T, Talja M, Taari K. Bacterial adherence to self-reinforced polyglycolic and acid and self-reinforced polylactic acid 96 urological spiral stents in vitro. Biomaterials 19(7-9): 677-681, 1998.

Pihlajamäki H, Böstman O, Tynninen O, Laitinen O. Long-term tissue response to bioabsorbable poly-L-lactide and metallic screws: an experimental study. Bone 39: 932-937, 2006.

Post JC. Direct evidence of bacterial biofilms in otitis media. Laryngoscope 111: 2083-2094, 2001.

Post JC, Stoodley P, Hall-Stoodley L, Ehrlich GD. The role of biofilms in otolaryngologic infections. Curr Opin Otolaryngol Head Neck Surg 12(3): 185-90, 2004.

Post JC, Hiller NL, Nistico L, Stoodley P, Ehrlich GD. The role of biofilms in otolaryngologic infections: update 2007. Curr Opin Otolaryngol Head Neck Surg 15: 347-351, 2007.

Qiu Y, Zhang N, An YH, Wen X. Biomaterial strategies to reduce implant-associated infections. Int J Artif Organs 30(9): 828-841, 2007.

Quirynen M, Marechai M, Busscher H, el-Abiad M, Arends J, van Steenberghe D. The influence of surface characteristics on the early bacterial colonization of intra-oral hard surfaces. J Clin Dent 1: 14-19, 1988.

Quirynen M, van der Mei HC, Bollen CM, Schotte A, Marechai M, Doornbusch GI, Naert I, Busscher HJ, van Steenberghe D. An in vivo study of the influence of the surface roughness of implants on the microbiology of supra- and subgingival plaque. J Dent Res 72(9): 1304-1309, 1993.

Rafferty MA, Siewerdsen JH, Chan Y, Moseley DJ, Daly MJ, Jaffray DA, Irish JC. Investigation of C-arm cone-beam CT-guided surgery of frontal recess. Laryngoscope 115: 2138-2143, 2005.

Ramakrishnan Y, Kotecha A, Bowdler DA. A review of retraction pockets: past, present and future management. J Laryngol Otol 121(6): 521-525, 2007.

Rangheard A-S, Marsot-Dupuch K, Mark AS, Meyer B, Tubiana J-M. Postoperative complications in otospongiosis: usefulness of MR imaging. Am J Neuroradiol 22: 1171-1178, 2001.

Ratcliffe A. Tissue engineering of vascular stents. Matrix Biol 19(4): 353-357, 2000.

Ratner BD. New ideas in biomaterials science – a path to engineered biomaterials. J Biomed Mater Res 27(7): 837-850, 1993.

Reck R, Helms J. The bioactive glass ceramic Ceravital in ear surgery. Five years´ experience. Am J Otol 6(3): 280-283, 1985.

Remuzzi A, Boccardo P. Albumin treatment reduces *in vitro* platelet deposition to PMMA dialysis membrane. Int J Artif Organs 16: 128-131, 1993.

Rice MA, Dodson BT, Arthur JA, Anseth KS. Cell-based therapies and tissue engineering. Otolaryngol Clin North Am 38(2): 199-214, 2005.

Robey TC, Välimaa T, Murphy HS, Törmälä P, Mooney DJ, Weatherly RA. Use of internal bioabsorbable PLGA “finger-type” stents in a rabbit tracheal reconstruction model. Arch Otolaryngol Head Neck Surg 126: 985-991, 2000a.

Robey TC, Eiselt PM, Murphy HS, Mooney DJ, Weatherly RA. Biodegradable external tracheal stents and their use in a rabbit tracheal reconstruction model. Laryngoscope 110: 1936-1942, 2000b.

Robinson S, Suomalainen A, Kortesniemi M. μ-CT. Eur J Radiol 56: 185-191, 2005.

Rokkanen PU, Böstman O, Hirvensalo E, Mäkelä EA, Partio EK, Pätiälä H, Vainionpää S, Vihtonen K, Törmälä P. Bioabsorbable fixation in orthopaedic surgery and traumatology. Biomaterials 21: 2607-2613, 2000.

Saidi IS, Biedlingmaier JF, Whelan P. In vivo resistance to bacterial biofilm formation on tympanostomy tubes as a function of tube material. Otolaryngol Head Neck Surg 120: 621-627, 1999.

Saint-Félix D, Trousset Y, Picard C, Ponchut C, Roméas R, Rougée A. In vivo evaluation of a new system for 3D computerized angiography. Phys Med Biol 39(3): 583-595, 1994.

Sanclement JA, Webster P, Thomas J, Ramadan HH. Bacterial biofilms in surgical specimens of patients with chronic rhinosinusitis. Laryngoscope 115: 578-582, 2005.

Santavirta S, Konttinen YT, Saito T, Grönblad M, Partio E, Kemppinen P, Rokkanen P. Immune response to polyglycolic acid implants. J Bone Joint Surg Br 72(4): 597-600, 1990.

Scarfe WC, Farman AG, Sukovic P. Clinical applications of cone-beam computed tomography in dental practice. J Can Dent Assoc 71(1): 75-80, 2006.

Scheuerman TR, Camper AK, Hamilton MA. Effects of substratum topography on bacterial adhesion. J Colloid Interface Sci 208: 23-33, 1998.

Schmidmaier G, Baehr K, Mohr S, Kretschmar M, Beck S, Wildemann B. Biodegradable polylactide membranes for bone defect coverage: biocompatibility testing, radiological and histological evaluation in a sheep model. Clin Oral Impl Res 17: 439-444, 2006.

Schulze D, Heiland M, Thurmann H, Adam G. Radiation exposure during midfacial imaging using 4- and 16-slice computed tomography, cone beam computed tomography systems and conventional radiography. Dentomaxillofac Radiol 33: 83-86, 2004.

Seibert JW, Danner CJ. Eustachian tube function and the middle ear. Otolaryngol Clin North Am 39(6): 1221-1235, 2006.

Semaan MT, Megerian CA. The pathophysiology of cholesteatoma. Otolaryngol Clin North Am 39(6): 1143-1159, 2006.

Siedentop KH, O´Grady K, Bhattacharyya TK, Shah A. Fibrin tissue adhesive and autologous concha cartilage for reconstruction of the posterior-superior canal wall of the chinchilla middle ear. Otol Neurotol 25(3): 220-222, 2004.

Siewerdsen JH, Daly MJ, Bakhtiar B, Moseley DJ, Richard S, Keller H, Jaffray DA. A simple, direct method for x-ray scatter estimation and correction in digital radiography and cone-beam CT. Med Phys 33(1): 187-197, 2006.

Smith JA, Danner CJ. Complications of chronic otitis media and cholesteatoma. Otolaryngol Clin North Am 39(6): 1237-1255, 2006.

Spengenberg C, Montie TC, Tümmler B. Structural and functional implications of sequence diversity of Pseudomonas aeruginosa genes oriC, ampC and fliC. Electrophoresis 19(4): 545-550, 1998.

Sobel JD, Obedeanu N. Role of hydrophobicity in adherence of gram negative bacteria to epithelial cells. Ann Clin Lab Sci 14(3): 216-224, 1984.

Spiegel JH, Kessler JL. Tympanic membrane perforation repair with acellular porcine submucosa. Otol Neurotol 26: 563-566, 2005.

Stamm G, Nagel HD. CT-expo – a novel program for dose evaluation in CT. Rofo 174(12): 1570-1576, 2002.

Stewart PS, Costerton JW. Antibiotic resistance of bacteria in biofilms. Lancet 358: 135-138, 2001.

Stickler DJ. Biofilms on catheters and urinary tract infections. Eur Urol Update Series 5: 1-8, 1996.

Stoor P, Grénman R. Bioactive glass and turbinate flaps in the repair of nasal septal perforations. Ann Otol Rhinol Laryngol 113(8): 655-661, 2004.

Stoor P, Söderling E, Andersson OH, Yli-Urpo A. Interactions between the frontal sinusitis-associated pathogen *Haemophilus influenzae* and the bioactive glass S53P4. Bioceramics 8: 253-258, 2006.

Štyriak I, Lauková A, Fallgren C, Wadström T. Binding of extracellular matrix proteins by animal strains of staphylococcal species. Vet Microbiol 67(2): 99-112, 1999.

Sukovic P. Cone beam computed tomography in craniofacial imaging. Orthod Craniofac Res 6 Suppl 1: 31-36; discussion 179-182, 2003.

Suomalainen A, Vehmas T, Kortesniemi M, Robinson S, Peltola J. Accuracy of linear measurements using dental cone beam and conventional multislice computed tomography. Dentomaxillofac Radiol 37: 10-17, 2008.

Suuronen R, Kallela I, Lindqvist C. Bioabsorbable plates and screws: current state of the art in facial repair. J Craniomaxillofacial Trauma 6(1): 19-27, 2000.

Suuronen R, Kontio R, Ashammakhi N, Lindqvist C, Laine P. Bioabsorbable self-reinforced plates and screws in craniomaxillofacial surgery. Biomed Mater Eng 14(4): 517-524, 2004.

Takahashi H, Iwanaga T, Kaieda S, Fukuda T, Kumagami H, Takasaki K, Hasebe S, Funabiki K. Mastoid obliteration combined with soft-wall reconstruction of posterior ear canal. Eur Arch Otorhinolaryngol 264(8): 867-871, 2007.

Tamai H, Igaki K, Kyo E, Kosuga K, Kawashima A, Matsui S, Komori H, Tsuji T, Motohara S, Uehata H. Initial and 6-month results of biodegradable poly-*l*-lactic acid coronary stents in humans. Circulation 102: 399-404, 2000.

Tammela TL, Talja M. Biodegradable urethral stents. BJU Int 92(8): 843-850, 2003.

Terekado M, Hashimoto K, Arai Y, Honda M, Sekiwa T, Sato H. Diagnostic imaging with newly developed ortho cubic super-high resolution computed tomography (Ortho-CT). Oral Surg Oral Med Oral Pathol Oral Radiol Endod 89(4): 509-518, 2000.

Tiainen J, Soini Y, Törmälä P, Waris T, Ashammakhi N. Self-reinforced polylactide/polyglycolide 80/20 screws take more than 1.5 years to resorb in rabbit cranial bone. Appl Biomater 70B: 49-55, 2004.

Truy E, Naiman AN, Pavillon C, Abedipour D, Lina-Granade G, Rabilloud M. Hydroxyapatite versus titanium ossiculoplasty. Otol Neurotol 28(4): 492-498, 2007.

Tu SJ, Shaw CC, Chen L. Noise simulation in cone beam CT imaging with parallel computing. Phys Med Biol 51(5): 1283-1297, 2006.

Tullis JL. Albumin. Background and use. JAMA 237(4): 355-360, 1977.

Törmälä P, Pohjonen T, Rokkanen P. Bioabsorbable polymers: materials, technology, and surgical applications. Proc Instn Mech Eng [H] 212(2): 101-111, 1998.

Törmälä P (ed.); Aho A, Anderson Ö, Heikkilä J, Keränen J, Konttinen Y, Lappalainen R, Lepojärvi M, Nevalainen J, Santavirta S, Salenius J, Tarvainen T, Törmälä P, Vallittu P, Viljanen V, Waris E, Waris V. Yleiskatsaus terveydenhuollon laitteissa ja tarvikkeissa käytettyihin biomateriaaleihin. Lääkelaitos, Helsinki, Finland, 2003: pp. 4, 9-10.

Uurto I, Mikkonen J, Parkkinen J, Keski-Nisula L, Nevalainen T, Kellomäki M, Törmälä P, Salenius J-P. Drug-eluting biodegradable poly-D/L-lactic acid vascular stents: an experimental pilot study. J Endovasc Ther 12: 371-379, 2005.

Uurto I, Kotsar A, Isotalo T, Mikkonen J, Martikainen PM, Kellomäki M, Törmälä P, Tammela TL, Talja M, Salenius J-P. Tissue biocompatibility of new biodegradable drug-eluting stent materials. J Mater Sci Mater Med 18: 1543-1547, 2007.

van Blitterswijk CA, Grote JJ. Biocompatibility of clinically applied hydroxylapatite ceramic. Ann Otol Rhinol Laryngol Suppl 144: 3-11, 1990.

van de Belt H, Neut D, Schenk W, van Horn JR, van der Mei HC, Busscher HJ. Infection of orthopedic implants and the use of antibiotic loaded cements. Acta Orthop Scand 72(6): 557-571, 2001.

Van Ongeval Ch. Digital mammography for screening and diagnosis of breast cancer: an overview. JBR-BTR 90(3): 163-166, 2007.

Verheyen CC, Dhert WJ, de Blieck-Hogersvorst JM, van der Reijden TJ, Petit PL, de Groot K. Adherence to a metal, polymer and composite by *Staphylococcus aureus* and *Staphylococcus epidermidis*. Biomaterials 14(5): 383-391, 1993.

Verhoeff M, van der Veen EL, Rovers MM, Sanders EA, Schilder AG. Chronic suppurative otitis media: a review. Int J Pediatr Otorhinolaryngol 70(1): 1-12, 2006.

Vincent R, Sperling NM, Oates J, Osborne J. Ossiculoplasty with intact stapes and absent malleus: the silastic banding technique. Otol Neurotol 846-852, 2005.

von Eiff C, Kohnen W, Becker K, Jansen B. Modern strategies in the prevention of implant-associated infections. Int J Artif Organs 28(11): 1146-1156, 2005a.

von Eiff C, Jansen B, Kohnen W, Becker K. Infections associated with medical devices: pathogenesis, management and prophylaxis. Drugs 65(2): 179-214, 2005b.

Vogt F, Stein A, Rettenmeier G, Krott N, Horffmann R, vom Dahl J, Bosserhoff AK, Michaeli W, Hanrath P, Weber C, Blindt R. Long-term assessment of a novel biodegradable paclitaxel-eluting coronary polylactide stent. Eur Heart J 25: 1330-1340, 2004.

Waris E, Konttinen YT, Ashammakhi N, Suuronen R, Santavirta S. Bioabsorbable fixation devices in trauma and bone surgery: current clinical standing. Expert Rev Med Devices 1(2): 229-240, 2004.

Watts S, Flood LM, Clifford K. A systematic approach to interpretation of computed tomography scans prior to surgery of middle ear cholesteatoma. J Laryngol Otol 114: 248-253, 2000.

Wiegert J, Bertram M, Netsch T, Wulff J, Weese J, Rose G. Projection extension for region of interest imaging in cone-beam CT. Acad Radiol 12(8): 1010-1023, 2005.

Wildemann B, Sander A, Schwabe P, Lucke M, Stöckle U, Raschke M, Haas NP, Scmidmaier G. Short term in vivo biocompatibility testing of biodegradable poly(D,L-lactide)-growth factor coating for orthopaedic implants. Biomaterials 26(18): 4035-4040, 2005.

Williams DF. A model for biocompatibility and its evaluation. J Biomed Eng 11(3): 185-191, 1989.

Williams MT, Ayache D. Imaging of the postoperative middle ear. Eur Radiol 14: 482-495, 2004.

Winter AA, Pollack AS, Frommer HH, Koenig L. Cone beam volumetric tomography vs. medical CT scanners. N Y State Dent J 71(4): 28-33, 2005.

Yamawaki T, Shimokawa H, Kozai T, Miyata K, Higo T, Tanaka E, Egashira K, Shiraishi T, Tamai H, Igaki K, Takeshita A. Intramural delivery of a specific tyrosine kinase inhibitor with biodegradable stent suppresses the restenotic changes of the coronary artery in pigs in vivo. JACC 32(3): 780-786, 1998.

Yamazaki K, Sato H, Murai K, Ogawa K. Infantile congenital cholesteatoma: A case report and literature review. Int J Pediatr Otorhinolaryngol 69(12): 1703-1707, 2005.

Yang WT, Carkaci S, Chen L, Lai CJ, Sahin A, Whitman GJ, Shaw CC. Dedicated cone-beam breast CT: feasibility study with surgical mastectomy specimens. Am J Roentgenol 189(6): 1312-1315, 2007.

Yates PD, Flood LM, Banerjee A, Clifford K. CT scanning of middle ear cholesteatoma: what does the surgeon want to know? Br J Radiol 75(898): 847-852, 2002.

Yung MW. Literature review of alloplastic materials in ossiculoplasty. J Laryngol Otol 117: 431-436, 2003.

Zdanowski Z, Ribbe E, Schalen C. Influence of some plasma proteins on in vitro bacterial adherence to PTFE and dacron vascular prostheses. APMIS 101(12): 926-932, 1993.

Ziegler CM, Woertche R, Brief J, Hassfeld S. Clinical indications for digital volume tomography in oral and maxillofacial surgery. Dentomaxillofac Radiol 31: 126-130, 2002.

ORIGINAL PUBLICATIONS